Identification and Analysis of Amino Acid Substitutions in Ebola Virus Glycoprotein Fusion Loop That Interfere With Infection

Identification and Analysis of Amino Acid Substitutions in Ebola Virus Glycoprotein Fusion Loop That Interfere With Infection

Sean Lowell Wilkes

A Thesis in the Field of Biology

for the Degree of Master of Liberal Arts

Harvard University

May 2012

Abstract

The Ebola virus glycoprotein, GP, is responsible for the fusion of the virus membrane with that of its host target and the consequent entry of the virus into the cell cytosol. GP is expressed on the surface of the virus membrane as a trimer of dimers, each of which is formed through the post-translational furin cleavage of native GP into two subunits: GP1, which contains a receptor binding domain, and GP2, which contains the spring-loaded fusion machinery. GP1 also acts as a clamp to hold GP2 in its pre-fusion conformation. Host factors trigger the release of the GP1 clamp and cause the metastable α-helix coiled-coil of GP2 to extend, inserting the fusion loop into the target membrane. The extended coil then folds back in on itself to form a highly stable six-helix bundle that is coupled to virus membrane fusion and infection. I hypothesize that amino acid residues with hydrophobic side changes that reside at the tip of the fusion loop are necessary for virus membrane fusion. To test this, the effects of substitutions in these residues on GP assembly and infection have been evaluated. I found that substitution of arginine for tyrosine 535 in GP2 did not affect glycoprotein synthesis, cleavage, virus incorporation, or host factor interactions but is highly defective for infection. These findings demonstrate that GP Y535 is essential for Ebola virus infection and that the Y535R mutant likely confers a defect in virus membrane fusion.

About the Author

Sean Lowell Wilkes is a career Army medical officer specializing in public health, biodefense, and infectious disease. He began his career as a preventive medicine science officer and environmental engineer at the U.S. Army Public Health Command. He has also served as a clinical investigator in the Democratic Republic of the Congo, and at the Pentagon as an Inspector General for the Department of Defense Detainee Program. In his last assignment, he served as the Commander of a medical brigade headquarters and headquarters company and as an emergency preparedness and contingency operations consultant to various federal, state and municipal agencies throughout the Northeast.

Sean holds a bachelor's degree in Neuroscience from Columbia University and a master's degree in Biotechnology with a concentration in Biosecurity and Biodefense from the University of Maryland.

For Mr. Gerald Voice. This is all your fault.

Acknowledgments

I would like to express my sincere gratitude to John Misasi, Marceline Côté, Anna Bruchez, and Tao Ren for the countless hours they spent training me and assisting me with tasks around the lab, not to mention their unfailing companionship throughout this whole ordeal. Thanks to Alexandra Bosse, Gabrielle Nekrasas, Nick Adams, Ryan Malone, and Mickey Segal for their enduring friendship and for being always knowledgeable and engaging sounding boards. And finally, a great deal of thanks to my thesis director, Dr. James Cunningham, without whose knowledge, guidance, and faith in my abilities I could never have achieved this. Thank you for making the leap and taking me on as your student.

Table of Contents

List of Tables

List of Figures and Graphs

Chapter I

Introduction

Viruses are infectious particles comprised of a nucleic acid core surrounded by a protein coat (Knipe & Howley, 2006). The diameter of spherical virus particles is 20 nm-300 nm (Collier et al., 1998), and filamentous particles may be as long as 1.4μm (Kuhn et al., 2010). The virus genome is located within the capsid, which is composed of one or a few virus-encoded proteins that assemble into icosahedral structures (Collier et al., 1998). For some viruses, the capsid is surrounded by a lipid bilayer derived from the host cell membrane. Embedded in the virus membrane (or envelope) are virus-encoded glycoproteins that mediate virus attachment and infection of host cells.

Viral Structure and Classification

The most basic foundation of virus classification is the composition of the nucleic acid core. Viral genetic material can be comprised of either RNA or DNA, and may be single or double-stranded. This is the basis for the Baltimore virus classification system, which organizes viruses into groups as depicted in Table 1 (Baltimore, 1971).

Group	Symbol	Description	Example
I	dsDNA	Double-stranded DNA	Poxvirus
II	ssDNA	Single-stranded DNA	Inovirus
III	dsRNA	Double-stranded RNA	Reovirus
IV	(+)ssRNA	Single-stranded RNA positive-sense	Calicivirus
V	(-)ssRNA	Single-stranded RNA negative-sense	Filovirus
VI	ssRNA-RT	Single-stranded RNA replicated through a DNA intermediate	Retrovirus
VII	dsDNA-RT	Double-stranded DNA replicated through an RNA intermediate	Caulimovirus

Table 1: Baltimore Classification of Viruses

Structurally, viruses may be divided into three basic classifications, based upon the organization of their capsid: Polyhedral, Helical, and Complex (Russell, Hertz, & McMillan, 2011).

Polyhedral viruses are formed by a nucleic acid core about which capsomeres are arranged to form a geometric shape such as an icosahedron.

Helical viruses contain a core of coiled nucleic acid that is surrounded by identical capsomeres arranged about the axis of the coil in a helix.

Complex viruses are those that can be classified as neither polyhedral nor helical. They may contain both polyhedral and helical structures, or other features such as multiple protein layers that coat the nucleic acid core.

Finally, viruses may be classified based on the presence or absence of an envelope. Non-enveloped viruses may take on any of the aforementioned forms. Such viruses are generated by the genetic machinery of their host and released upon lysis of the infected cell. Some, however, exit the cell through an exocytotic process known as budding. These viruses leave their hosts surrounded by a segment of the cell's lipid outer membrane and are thus classified as enveloped.

Viral Entry, Replication, and Release

Viruses are obligate intracellular parasites, and therefore must exploit the cellular machinery of host organisms in order to replicate (Flint et al., 2009). This requires the virus to first transport their genetic material across the cell membrane and into the cell. Viruses make use of a variety of mechanisms to do this, but there are some commonalities between them.

Before entering the cell a virus first attaches to the membrane surface. This is achieved through binding to a cell surface structure, such as a protein, which may fall into one of two categories: attachment factors or receptors (Knipe & Howley, 2006). Structures of the former type function merely as a substrate to which the virus may adhere, granting it sustained proximity to the cell and an opportunity to achieve entry. The latter type, receptors, may or may not serve to fasten the virus to the cell surface, but all function to actively promote entry, either by initiating endocytosis, activating cell signaling pathways, or inducing the interacting viral protein to alter conformation.

A wide variety of attachment factors and receptor configurations exist, from carbohydrates and proteoglycans to membrane transport proteins and signaling peptides (Young, 2001). Once bound, an active receptor typically activates a mechanism to either internalize the virus or to transport the virus or its genetic material across the cell membrane and into the cytosol (Sieczkarski & Whittaker, 2005). Some receptors act alone, but others function in conjunction with co-factors or co-receptors to grant the virus entry. As with the primary receptors, co-receptors and co-factors may serve a variety of functions. In some instances, for example, they perform an enzymatic reaction that acts to trigger a virus's fusion mechanism. In others cases the co-factor has been shown to cleave surface proteins or otherwise alter their conformation and thereby make the receptor binding domain accessible to the target receptor.

Once the entry mechanism has been activated a virus will typically penetrate membrane either through fusion of its membrane with that of the cell or via physical disruption of the cell membrane (Earp et al., 2005). For enveloped viruses this may occur on the cell surface or after uptake via endocytosis, while non-enveloped viruses typically gain access to the cytosol only

after endocytic uptake. The specifics of viral entry via membrane fusion will be detailed further later in this chapter.

Uncoating

After the virus has gained access to the cell cytosol it must open or disassemble the protein capsid in order to release its genetic material to the cell's expression and replication machinery. This process is known as uncoating and may occur simultaneously with membrane fusion or entry, or once it has completely entered the cell (Helenius, 2006). Occassionally uncoating is initiated upon binding to the virus receptor, as is the case with polio (Racaniello, 1996), while in other instances the process requires assistance from host proteins, which is true of many poxviruses (Butel, 2010). Ebola virus makes use of its own RNA-dependent RNA polymerase (RdRp) to initiate a partial uncoating and grant the polymerase access to the genome (Ahlquist, 2002).

Transcription, translation, and replication can also take many forms, dependent in large part upon the class of genetic material present within the virus. In short, the viral genome is replicated while mRNA is transcribed, either by the virus's own polymerase or the replication and transcription machinery of the infected cell, and is directed towards ribosomes for translation (Ball, 2006). Some viruses, such as dsDNA viruses, require their genetic material to be transported to the nucleus for replication and transcription by the cell's nuclear enzymes while for others, like many (+)ssRNA viruses, the genetic material is immediately replicated by the virus's own polymerase upon uncoating and translated by host ribosomes. Retroviruses convert their RNA into DNA through the application of their own reverse transcriptase enzyme and then utilize another enzyme, integrase, to incorporate the DNA into the host genome. The host then

expresses the incorporated genes and the viral DNA is replicated by the host during cell replication as a permanent component of the host genome. As a negataive sense (-)ssRNA virus, Ebola must first have its genome transcribed by RdRp to convert it into a positive sense RNA that can be read by host ribosomes (Ahlquist, 2002). Host ribosomes then translate the various proteins the virus required. When one of these, the nucleocapsid, reaches a certain concentration within the cell the function of RdRp shifts from transcription to replication of the (-)ssRNA.

The proteins expressed throughout this process usually include structural components like capsid and envelope proteins, proteins and enzymes required for assembly such as viral matrix proteins, and those proteins and enzymes that the virus will need upon infection of its host, like polymerase (Ball, 2006).

Once the viral mRNA is translated into proteins by the ribosomes these proteins are post-translationally processed, membrane bound proteins are glycosylated, and the proteins are directed to the virus assembly site through associated sorting signals. The replicated viral nucleotides are packaged within the virion, often due to the presence of a packaging signal within the nucleotide sequence. In retroviruses this packaging signal is a cis-acting RNA element referred to as ψ (Bannert, Fiebig, & Hohn, 2010).

After assembly the virus is released, a process that is most commonly accomplished through one of three mechanisms: cell death, exocytosis, or budding (Pe'ery & Mathews, 2006). Some viruses will simply induce cell lysis, by opening pores in the cell surface with viroporins or digesting it with lysozymes, effectively forcing their way out of a cell and killing it in the process, while others will induce a cell to undergo controlled cell death, or apoptosis, by generating associated signals such as the activation of host caspases. Viruses may make use of the host's exocytosis pathway to encase the virus in vacuoles which are then transported to the

cell surface, merge with the membrane, and release the virus into the lumen. Enveloped viruses frequently follow another route. These viruses produce membrane-bound surface proteins that are transported by the cellular machinery to the surface. Then, by assembling the viral components near the cell surface and inducing the viral envelope protein-laden cell membrane to form an envelope around them, the virus ejects itself by causing the surrounding membrane envelope to bud off from the cell (Hunter, 2006).

Entry Receptors

Viruses utilize a wide array of strategies in order to gain access to the interior of the cell, often adapted to the uptake mechanisms and structural properties of the host cell. As noted previously, the virus must attach to the cell surface first, either through interactions with attachment factors or with specific receptors (Table 2). After attachment, non-enveloped viruses may force their way into the cell by penetrating the cell membrane or cell wall and injecting the nucleic acid core into the cell cytoplasm (Sebestyén et al., 2006). They may also activate the cell's endocytosis machinery, be taken up into the cell inside a vacuole, and then either penetrate the vacuole membrane or get released by the host into the cytosol (Mercer, Schelhaas, & Helenius, 2010). Enveloped viruses, on the other hand, often make use of their own surrounding membranes to gain access to the cell by fusing it with the cell membrane, merging the contents of the virus with the cytosol (Harrison, 2008). Some enveloped viruses require a receptor to initiate this fusion process.

Virus binding to attachment factors is generally weak and non-specific. The individual binding interaction between a virus and a given attachment factor tends to be of low affinity, but

this is frequently overcome through the accumulation of multiple binding interactions occurring at the same time, resulting in firm adherence (Marsh & Helenius, 2006). Viruses often demonstrate affinity for cell surface lipids or carbohydrates, and common attachment factors include heparin sulfate and sialic acid (Hulo et al., 2011).

Virus receptors frequently take the form of membrane-bound or transmembrane proteins, particularly in the case of those that actively facilitate viral entry. Beyond attachment, these proteins may act to internalize a bound virion through activation of a cell signaling pathway. For example, the reovirus first attaches to sialic acid but is then thought to be internalized through the triggering of endocytosis and facilitation of trafficking by β1 integrins (Maginnis et al., 2008; Maginnis et al., 2006). In addition to signaling the cell to internalize the virus, transmembrane receptors may also act to trigger a virion's own entry machinery. This is the case for some enveloped viruses such as Nipah virus, wherein the G-protein fusion mechanism is triggered by the binding of G to EFNB2 or EFNB3 (Mizra et al., 2011).

As previously noted, some viruses have an affinity for carbohydrates, thus those surface proteins that have been glycosylated (glycoproteins) are particularly ripe targets for attachment, and certain viruses may in-fact bind to the carbohydrate side chains of these molecules rather than a particular active site within the protein itself as it acts to facilitate entry (Eckert & Kim, 2001).

Entry Pathways

Viruses are able to take advantage of a number of different pathways in order to gain entry into the cell. Some viruses may enter their host target on the cell surface, a pathway that is particularly suited to enveloped viruses as they are able to merge with the cell membrane and avoid damaging the surface of the cell in a way that would expose the cytosol to the cell exterior and potentially result in cell death (Harrison, 2008). Others enter after internalization via cellular transport mechanisms, gaining access to the cytoplasm from within a vesical such as an endosome or lysosome (Mercer, Schelhass, & Helenius, 2010). The four most common mechanisms include cell surface entry, clathrin-mediated entry, calveola-mediated entry, and macropinocytosis.

Cell Surface Entry

Some enveloped viruses are able to gain entry to the cell immediately upon coming into contact with the cell surface. As noted above an enveloped virion is necessary as non-enveloped viruses typically gain entry through the physical disruption of the plasma membrane. Such a disruption of the membrane at the cell surface would cause the cell cytoplasm to be brought into contact with the surrounding external environment and could induce apoptosis. But an enveloped virion can avoid this by fusing its membrane with that of its target host. Viruses that tend to engage in this entry pathway include those of families retroviridae and herpesviridae (Lavillette et al., 2000; Spear & Longnecker, 2003). This method of entry is usually triggered through receptor binding. Though this entry pathway may appear to be the most direct, it does present the risk of immune system recognition, since upon membrane fusion the proteins present on the viral surface will have been integrated into the cell membrane.

Virus	Viral Protein	Receptor/Factor	Entry Pathway
RNA VIRUSES			
Ebola virus	Envelope GP	NPC-1	Macropinocytosis and host cell membrane fusion
Influenza B virus	HA	Sialic acid	
Influenza C virus	HE	Sialic acid	
Influenza A virus	HA	Sialic acid	Clathrin-mediated and clathrin/ caveolin-independent endocytosis
Lassa virus	Glycoproteins	α-dystroglycan	Clathrin/caveolin-independent endocytosis
Junin virus	Glycoproteins	TFRC	Clathrin-mediated endocytosis
Machupo virus	Glycoproteins	TFRC	Clathrin-mediated endocytosis
Nipah virus	Glycoprotein G	EFNB2, EFNB3	Clathrin-mediated endocytosis and Host cell membrane fusion
Dengue virus	Env. Protein E	Heparan sulfate	Clathrin-mediated endocytosis
Enterovirus	VP1, VP2, VP3	CD55, sialic acid	
Hepatitis C	E1 and E2	Heparan sulfate, LDLR, CD81	Clathrin-mediated endocytosis
Coxsackievirus B1-B6	VP1, VP2, VP3	CXADR	Macropinocytosis
DNA VIRUSES			
Parovirus B19	VP1, VP2	Globoside, Integrin α5 β1	Clathrin-mediated endocytosis
Vaccinia virus	D8, H3, A26 A27	Laminin, Heparan sulfate	Macropinocytosis
Adenovirus A, C, D,E F	Penton protein, Fiber protein,	Integrin αV, CXADR	Clathrin-mediated endocytosis
Herpes simplex 1	Glycoproteins gB, gC, gD	Heparan sulfate, PILRA, PVRL1 TNFRSF14	Host cell membrane fusion
Simian virus 40	VP1, VP2, VP3	Gangliosides, MHC class I	Caveolin-mediated endocytosis
Epstein-Barr	gp350/220, BMRF2	CR2	Host cell membrane fusion
RETROVIRUSES/PARARETROVIRUSES			
HIV-1 types 1, 2	Envelope gp120 Envelope gp41	CD4, CXCr4, CCr5, Hep. sulf., glycosphingolipid	Clathrin-mediated endocytosis
SIV	Envelope GP	CD4	
Hepatitis B virus	Large envelope protein	Heparan sulfate	Caveolin-mediated endocytosis

Table 2: Virus binding proteins, receptors and attachment factors, and entry pathways (Mercer & Helenius, 2009; Hulo et al., 2011; Nanbo et al., 2010).

Clathrin-Mediated Entry

Endocytosis via the clathrin-mediated pathway is among the most common means of entry for viruses, both enveloped and non-enveloped alike. Viral entry into the cytosol typically

occurs after complete uptake into the endosome, followed by a reduction in pH that triggers an entry mechanism such as membrane fusion. This pathway is so named because it involves the formation of small vesicles that are coated in a complex of clathrin and associated proteins in the form of a lattice (Fotin et al., 2004). The process often begins with clathrin-coated pits, partially invaginated membrane structures containing pre-assembled clathrin complexes, the components of which work in concert upon activation to initiate endocytosis (Schmid, 1997; Mercer, Schelhaas, & Helenius 2010). This process may be stimulated by a simple physical interaction between virion particles and this structure. In other instances the formation of the clathrin complex is induced by the interaction of the virus with other structures on the target membrane (Cureton et al., 2009). Upon uptake the vesicles fuse with early endosomes and the virus proceeds down the endocytic pathway until an entry mechanism, such as fusion, is triggered (Doherty & McMahon, 2009; Mercer, Schelhaas, & Helenius, 2010).

Caveolae-Mediated Entry

Another important route of endocytic uptake involves calveolin and the formation of lipid rafts. This caveolae-mediated pathway is common among polyomaviruses such as Simian vacuolating virus 40 (SV40) (Hulo et al., 2011). The pathway begins with caveolae, specialized constructs of the cholesterol- and shingolipid-enriched microdomains known as lipid rafts that have formed invaginations and contain clusters of receptors and signaling molecules involved in uptake (Anderson, 1998; Mercer, Schelhaas, & Helenius, 2010). The internalization process is triggered by binding to a ligand, such as the carbohydrate moiety of a ganglioside in the case of SV40, and the newly formed complex then relocalizes to the caveolae, generating a trans-membrane signal that induces a signaling cascade to initiate the formation of a vesicle and

uptake of the bound virus (Pelkmans, Kartenbeck, & Helenius, 2001; Pelkmans & Helenius, 2002; Ewers et al., 2010).

Macropinocytosis

This route of celluar uptake is focused on the internalization of fluids on a large scale. It is a non-specific process that utilizes the growth factor-induced and actin-dependent formation of large extracellular fluid-filled vesicles known as macropinosomes (Mercer & Helenius, 2009). Because it is not driven by a particular ligand interaction or membrane-bound structure the vacuole is large and irregular, formed through the activation of actin, the deoupling of the cytoskeleton, and the consequent ruffling of the plasma membrane into lamellipodia, filopodia, and blebs (Mercer, Schelhaas, & Helenius, 2010). Viruses that have been shown to utilize this largely indirect method of entry include vaccinia virus, coxsackievirus group B, and HIV-1, as well as Ebola virus (Mercer & Helenius, 2009; Nanbo et al., 2010).

Viral Fusion and Fusion Mechanisms

Once cellular uptake has occurred viruses still must penetrate the plasma membrane to gain access to the cytosol where it can then access the cellular machinery and begin to replicate. As noted previously, enveloped viruses have the advantage of being enclosed in a lipid bilayer much like the plasma membranes of their host targets. Thus, enveloped viruses are able to enter the cell through a process of membrane fusion, wherein the lipid bilayers of the virus and the cell are brought into close proximity such that they merge to become a single, contiguous membrane.

The viral fusion process is mediated by one or more fusion proteins, many of which have been identified and characterized (Harrison, 2008). These proteins and their viruses may be categorized into any one of three classes.

Class III Fusion Proteins

Class III fusion protein viruses include Epstein-Barr virus (EBV) and Herpes Simplex virus 1 (HSV-1), for which the fusion protein is known as gB, and Vesicular Stomatitis Virus (VSV), for which the fusion protein is known as G (Backovic & Jardetzky, 2009). Proteins of this class are comprised of five distinct domains: a fusion domain (I) that leads into a pleckstrin-like fold-containing domain with two β-strands (II), followed by a helix-dominated domain (III), followed by a β-strand-heavy domain (IV) and, finally, the C-terminus domain (V). Monomers of the class III, once expressed, form trimers on the envelope surface. The fusion domain is an extended β-sheet structure that presents, at its tip, two disorganized loop structures containing hydrophobic residues. Together, the loops are thought to comprise the fusion peptide that is inserted into the target membrane. The pleckstrin-like fold of domain II is suspected to serve as a binding site for phospholipids and may be involved in triggering the fusion mechanism of the protein. Domain III contains a long α-helix that, when joined with those of the protein's monomer counterparts, forms the coiled-coil that serves as the core of the resultant trimer structure. Domain V also appears to function as a site of interface in trimerization, while domain IV is a highly flexible domain predominantly comprised of β-sheets.

In the pre-fusion conformation, the fusion loops of the fusion domain are initially oriented towards the viral envelope. The triggering of the fusion mechanism, resulting from a reduction of pH in the case of VSV-G, causes the fusion domain to extend upward while

domains II through V reorient towards the envelope surface. Of the five domains, only domain III undergoes a significant degree of refolding during this process, while the others largely maintain their pre-fusion structures. As the mechanism continues along its course, the c-terminus domain and fusion domain then fold towards one another, bringing the two adjoined membranes into proximity, allowing them to fuse and a pore to open.

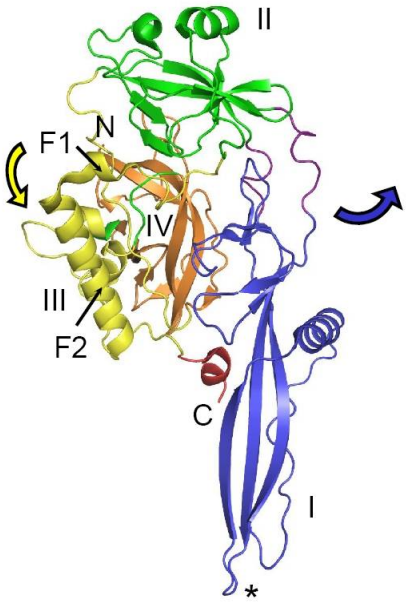

Figure 1: The pre-fusion structure of the VSV G fusion protein (Backovic & Jardetzky, 2009) illustrating domains I, II, III, IV, and C (V), as labeled. Domain I, in blue, is the fusion domain. Domain III, in yellow, experiences significant refolding during the conformational change that results in membrane fusion. The purple unstructured regions between domains I and II serve as the hinge about which domain I folds to extend upward into the host target membrane.

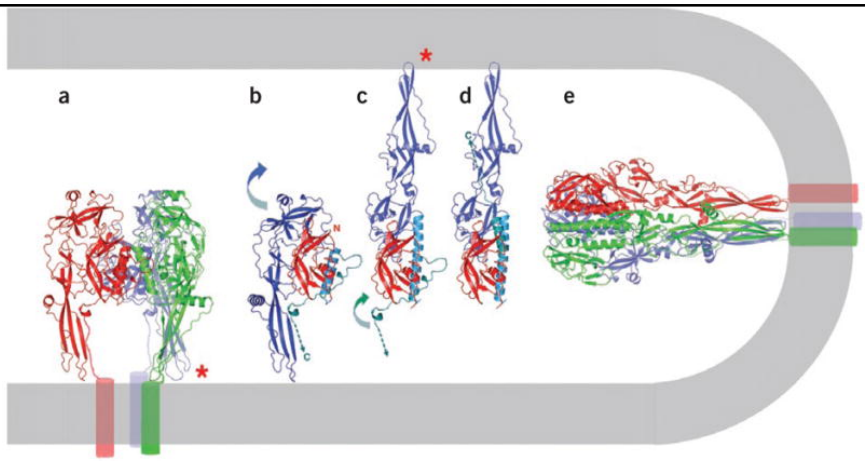

Figure 2: Depiction of the sequence of conformational changes that are thought to occur in VSV-G in the course of fusing the viral envelope with the target host membrane (Harrison, 2008). Step (a) illustrates the pre-fusion conformation of the VSV-G trimer. Step (b) shows the pre-fusion monomer, with an arrow indicating the path along which the fusion domain will fold upon the initiation of fusion. Step (c) is the extended intermediate, at which point the dual-looped fusion peptide has inserted into the target membrane. The arrow illustrates the direction that the c-terminal domain V will fold to complete the fusion process. Step (d) shows the post-fusion conformation of a single subunit while (e) shows the full post-fusion trimer and illustrates the manner in which the protein fuses the two adjoined membranes together.

Class II Fusion Proteins

Class II fusion protein viruses include alphaviruses and flaviviruses (Kielian, 2006). These enveloped viruses contain surface fusion proteins known as E proteins, as well as regulatory companion proteins. For alphavirus this companion protein is known as PE2, while for flavivirus it is called prM. These regulatory proteins are eventually post-translationally processed into mature versions (E2 and M respectively in the aforementioned examples) and dimerize with their E protein counterparts. They then collectively trimerize to form a working fusion protein.

The class II fusion proteins are elongated rod-shaped molecules with two β-barrel masses at one end. The opposite end of the rod-shaped structure is comprised of a conserved loop containing hydrophobic residues that may be readily inserted into a lipid membrane.

In its pre-fusion state the E protein forms a dimer in which the hydrophobic fusion loop region of each are nestled into the domain III structure of the other. When the fusion mechanism is

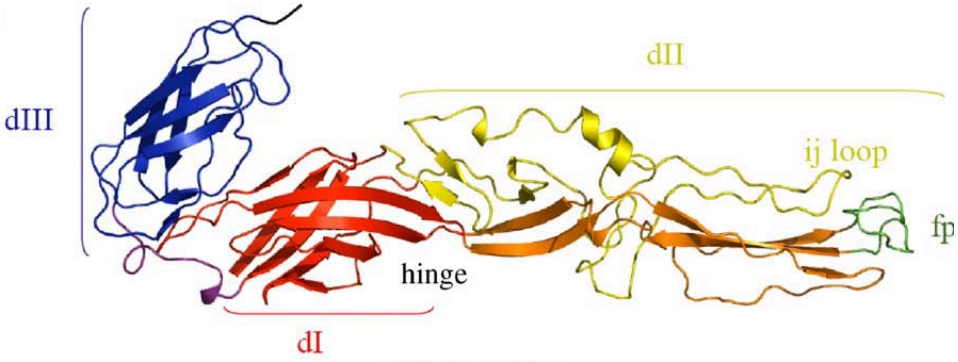

Figure 3: The pre-fusion structure of flavivirus E protein monomer (Kielian, 2006). The red and blue domains I and III are the two β-barrels. The yellow and orange domains comprise the rod-shaped extension at the tip of which resides the fusion loop, depicted in green, that is inserted into the target host membrane.

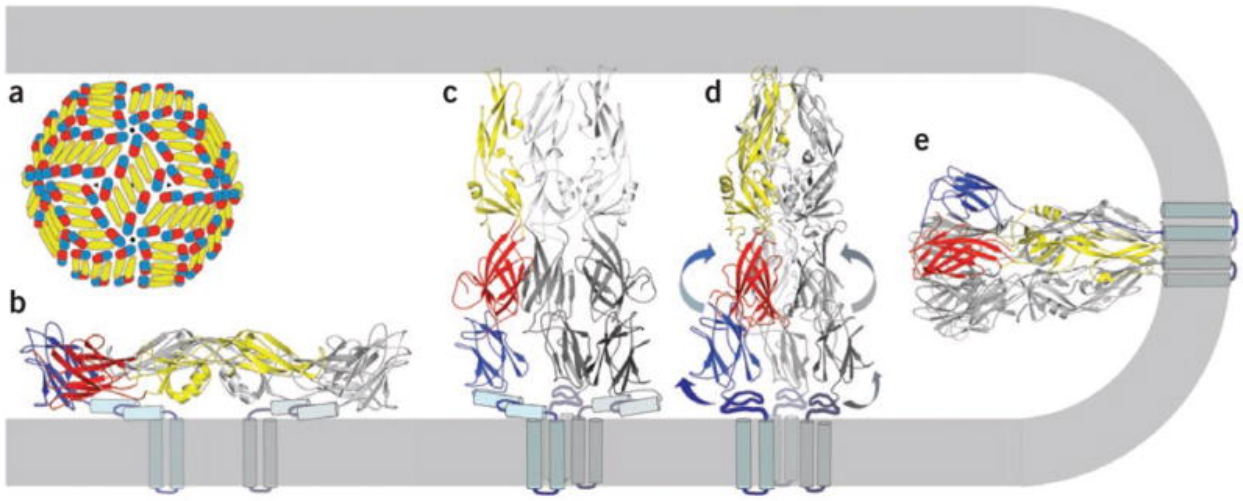

Figure 4: Depiction of the sequence of conformational changes that occur in flavivirus E protein in the course of fusing the viral envelope with the target host membrane (Harrison, 2008). Step (a) shows how 90 distinct E protein dimers are packed together on the surface of the flavivirus virion in the form of an icosahedron. Step (b) illustrates the pre-fusion conformation of a single E protein dimer, while (c) is the extension of the E protein fusion loop, a process during which the monomers, having dissociated from their dimers, start to reform as a trimer. Step (d) depicts the extended intermediate, at which point the trimer is fully formed and domains I and II are pulled inward toward the core. Finally, (d) demonstrates the conformation of the protein after domain III has folded upward towards the fusion loop, merging the two bound membranes together.

triggered–in the case of alphaviruses and flaviviruses by a reduction in pH after endocytic uptake–a conformational change is initiated wherein the dimer dissociates, exposing the fusion loop, which then inserts into the target membrane in a cholesterol-dependent manner. As this occurs the E protein monomers re-associate into trimers. While the stem region of this trimeric

structure is highly ordered, class II proteins do not form the more stable coiled-coil structure seen in class I proteins. Once the fusion peptide inserts and the trimer forms, the protein folds inward, around a hairpin secondary structure until the adjoined membranes become fused, allowing a pore to form.

Class I Fusion Proteins

Considerable progress has been achieved in understanding the mechanism of class I virus glycoprotein-mediated membrane fusion and infection (Harrison, 2008). In particular, it has been observed that there is a great deal of structural and functional similarity in the glycoproteins of otherwise unrelated viruses such as orthomyxoviruses (influenza), retroviruses (HIV), paramyxoviruses (Nipah, Hendra virus), filoviruses (Ebola virus), coronaviruses (SARS) and arenaviruses (lassa fever virus) (Figure 5). Our current understanding of the role of these proteins in entry has largely been achieved through the studies of hemagluttinin HA0 (Figure 6), the glycoprotein that mediates entry of influenza virus particles into cells (reviewed by White et al., 2009). In infected cells, HA0 is synthesized in the rough ER and rapidly assembles into trimers. After transport to the Golgi apparatus, HA0 is glycosylated and then cleaved by the cellular protease furin into HA1 and HA2 subunits, which remain associated (Lazarowitz, Compans, & Choppin, 1971; Skehel & Waterfield, 1975). After cleavage and transit to the plasma membrane, the mature HA1/HA2 trimers are incorporated into budding virus particles.

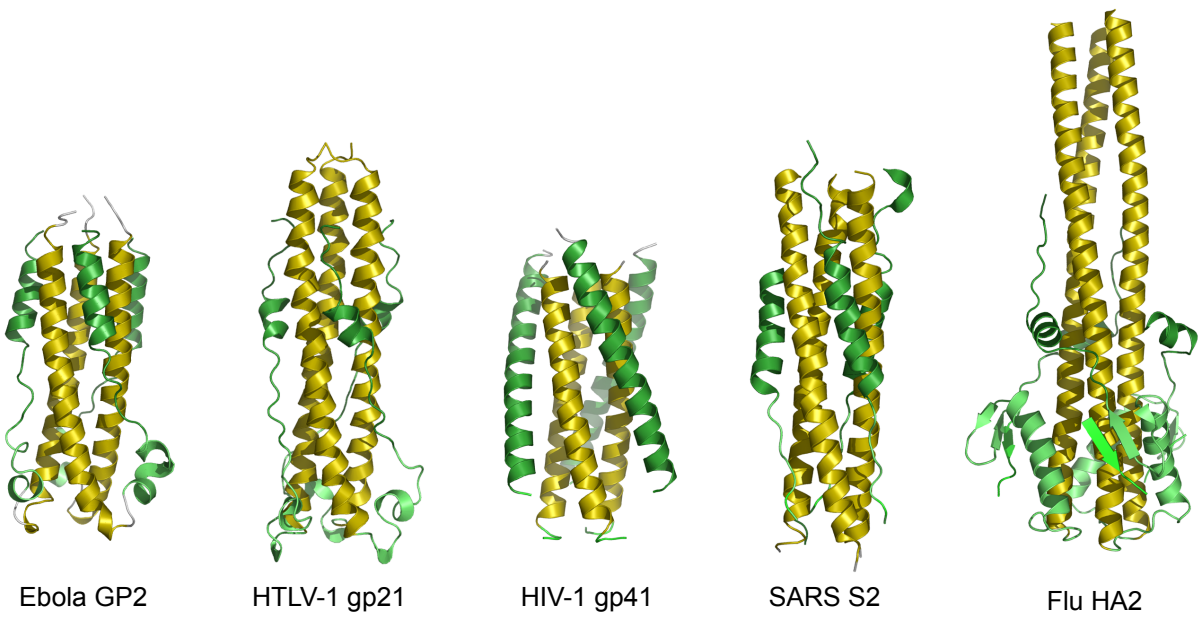

Figure 5: Six stranded helical bundle is conserved feature of post-fusion conformation of transmembrane domain of EboV, HTLV-1, HIV, SARS, and influenza membrane glycoproteins. The post-fusion six-helix bundle structure of class I fusion peptides is shown. In the metastable pre-fusion, the second set of helices (green) is folded into the first (yellow) in a hairpin turn and locked into place with the clamp of the binding subunit (not shown). This metastable structure serves as the spring that, when triggered, drives the fusion peptide into the host target membrane. The subsequent formation of the six helix bundle then pulls the adjoined membranes together until they fuse.

The atomic resolution structures of pre-fusion HA and post-fusion HA2 have been determined (Wilson et al., 1981) (Figures 1 & 2). In the prefusion structure, the transmembrane subunit HA2 forms a three-stranded coiled coil that mediates trimerization (Wilson et al., 1981). The site of furin cleavage is a loop that projects outward from the trimer, allowing access to it for proteolysis (see Figure 6, arrow 2) (Chen et al., 1998). Substantial progress has been made in understanding how mature HA mediates infection. The attachment of influenza particles to cells is mediated by residues at the top of HA1 that bind to sialic acids on host membrane glycoproteins (Gottschalk, 1959; Bergelson et al., 1982; Wiley & Skehel, 1987). The sialic acid

within a shallow pocket at the distal end of HA1 (see Figure 6, arrow 3) (Wilson, Skehel, & Wiley, 1981; Weis et al., 1988; Nobusawa et al., 1991; Kelm et al., 1992; Sauter et al., 1992; Watowich, Skehel, & Wiley, 1994; Eisen et al., 1997; Martín et al., 1998).

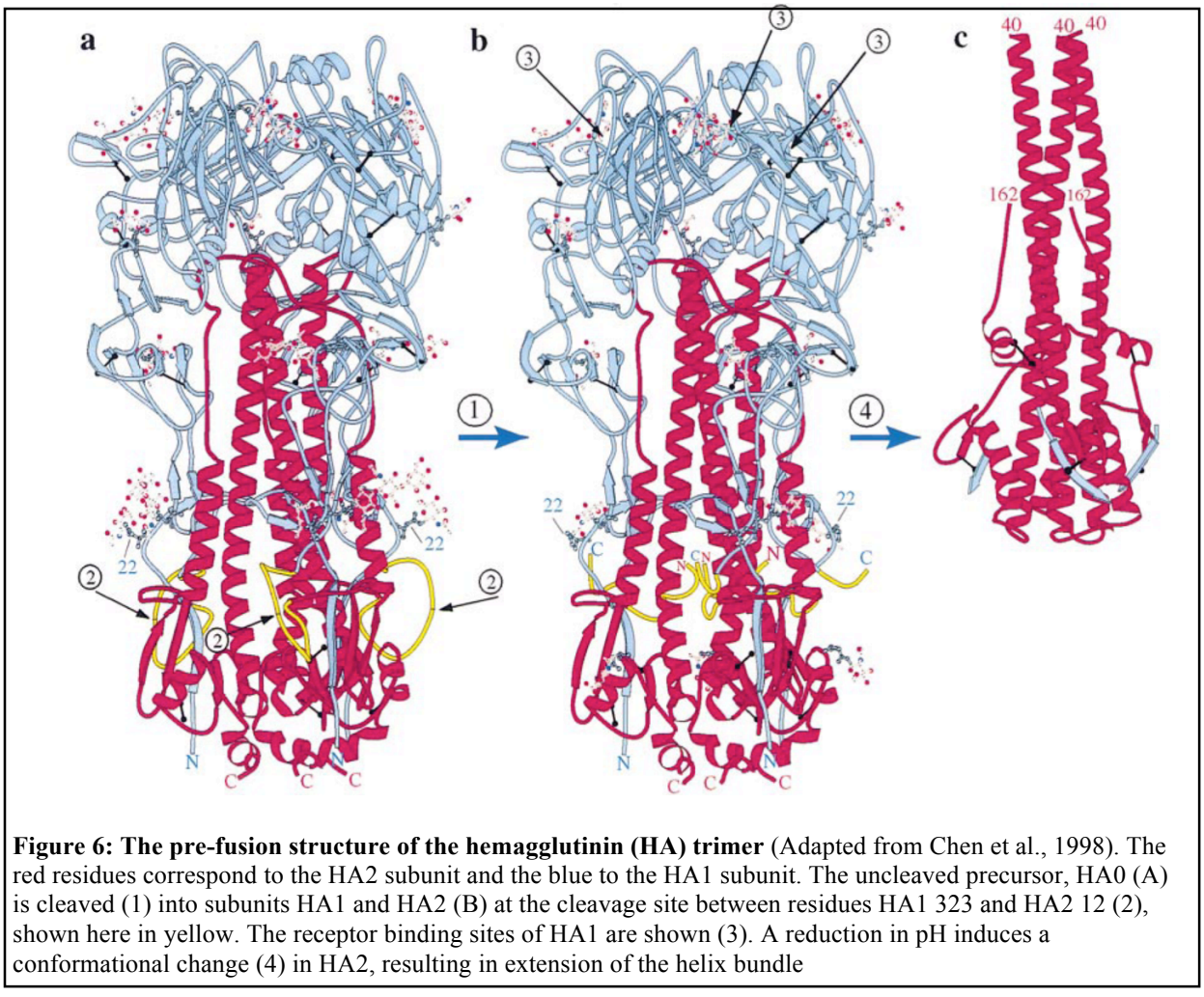

Figure 6: The pre-fusion structure of the hemagglutinin (HA) trimer (Adapted from Chen et al., 1998). The red residues correspond to the HA2 subunit and the blue to the HA1 subunit. The uncleaved precursor, HA0 (A) is cleaved (1) into subunits HA1 and HA2 (B) at the cleavage site between residues HA1 323 and HA2 12 (2), shown here in yellow. The receptor binding sites of HA1 are shown (3). A reduction in pH induces a conformational change (4) in HA2, resulting in extension of the helix bundle

The structural details of the conformational changes in HA associated with infection are summarized in Figure 7. After attachment to sialic acid-containing membrane glycoproteins, influenza particles are taken up into cell vesicles by endocytosis (Lakadamyali, Rust, & Zhuang, 2004). Virus containing endosomes are acidified by cell proton pumps and the reduction in pH

to <6.0 induces a conformational change in HA2 (Skehel et al., 1982; Doms, Helenius, & White, 1985; Bullough et al., 1994), (Huang, Rott, & Klenk, 1981). Two key steps in the conformational change have been identified. First, Carr and Kim showed that an unstructured loop is converted to an alpha helix at acid pH (Wiley & Skehek, 1987; Carr & Kim, 1993). They proposed that this conformational change would result in the formation of an extended strand in which the N-terminal portion of HA2 was exposed (see Figure 7c). Functional studies reveal the residues within the exposed N-terminal domain of HA2 penetrate the membrane of the target cells (Daniels et al., 1985; Gething et al., 1986; Düzgüneş & Gambale, 1988; Rafalski et al., 1991). Second, it was shown that the extended conformation undergoes an additional conformational change due to the formation of a hairpin loop near the middle of the HA2 stalk such that the domain adjacent to the virus membrane folds back onto the outer surface of the central trimeric coiled coil (Figure 7d) (Wiley, 1994). As a consequence of the formation of the helical bundle, the cell membrane containing the N-terminal domain is pulled into close proximity with the virus membrane. Although not fully understood, fusion of the virus and host membranes is coupled to hairpin formation and results in the creation of a membrane pore that is the conduit for transfer of the virus capsid/genome into the cytoplasm of the cell (Harrison, 2008).

Carr and Kim observed that exposure of HA to either heat or urea induces the conformational change from pre-fusion to post-fusion HA2 and this conversion is irreversible and inactivates virus infection (Carr, Chaudhry, & Kim, 1997). Moreover, the post-fusion conformation of HA2 is highly resistant to denaturing conditions or heating, indicating it is highly stable. Based on these findings, they proposed the “spring-loaded” model of infection (illustrated in Figure 8) to assert that pre-fusion HA2 is metastable, that it is held in place by the

HA1 “clamp,” and that fusion is triggered by acid pH-dependent reduction in the threshold to complete refolding of HA2 into most stable low energy conformation (Figure 7e) (Carr & Kim, 1993; Tatulian et al., 1995; Carr, Chaudhry, & Kim, 1997). Thus, the function of low pH in

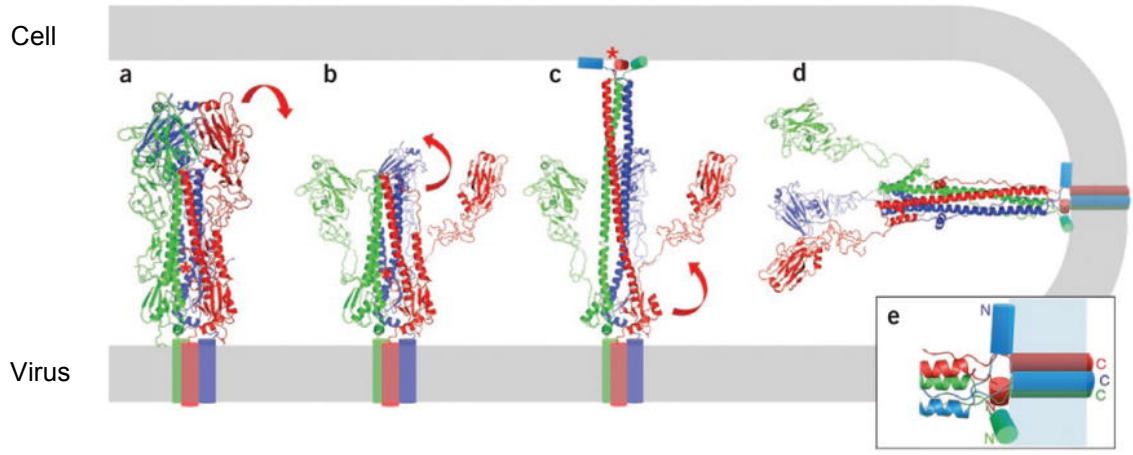

Figure 7: Depiction of the sequence of conformational changes that occur in influenza hemagglutinin in the course of fusing the viral envelope with the target host membrane (Adapted from Harrison, 2008). Step (a) illustrates the pre-fusion conformation, (b) shows the dissociation of HA1 triggered by a reduction in pH and the binding of protons, (c) is the extension of the helical region of the transmembrane domain containing the hydrophobic fusion peptide at its tip, and (d) demonstrates the conformation of the protein after the helix has folded back in on itself and has merged the two bound membranes together.

infection is to remove constraints on the folding of pre-fusion HA2 conferred by its close association with HA1.

As noted above, structural and functional studies indicate that the spring-loaded mechanism has also been adopted by retroviruses (HIV), paramyxoviruses (Nipah, Hendra virus), filoviruses (Ebola virus), coronaviruses (SARS) and arenaviruses (lassa fever virus) (White et al., 2008). In the most well studied case, sequential binding to host membrane

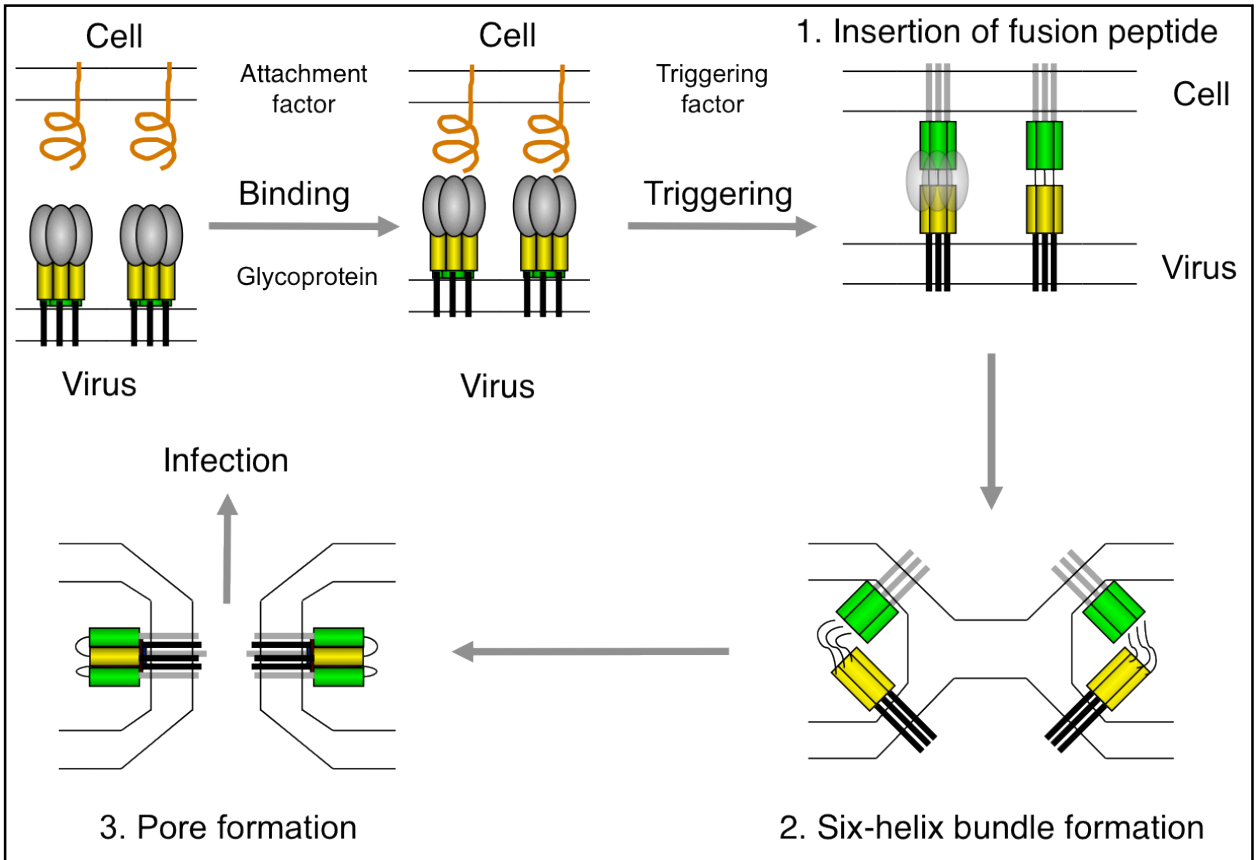

Figure 8: Spring-loaded model of class I fusion protein mechanism. The first subunit of the glycoprotein binds to its target attachment factor or receptor. One or more triggering factors causes a conformational change in the subunit, resulting in a release of its clamp on the second subunit and triggering the spring-loaded extension of the coiled-coil stem into the target membrane. The coiled coil then continues on an energetically favorable path, folding back in on itself to form a highly stable six-helix bundle, and bringing the two adjoined membranes into closer proximity. This permits lipid mixing, fusion, and the eventual formation of a pore through which the virus may pass.

receptors CD4 and CXCR5 provides the signal that initiates the refolding of the metastable pre-fusion HIV envelope glycoprotein that is required for membrane fusion and infection (Feng et al., 1996; Dragic et al., 1996; Lu et al., 1997; Sullivan et al., 1998; Berger, Murphy, & Farber, 1999; Gallo et al., 2003). CD4 and CXCR4 are expressed on helper T cells and it is the premature loss of these cells in HIV infection that underlies the immunosuppression that is the central feature of AIDS (Moore et al., 2004). Thus, identification of the host factors that trigger

the conformational changes in virus glycoproteins that mediate infection may illuminate underlying pathways of virus transmission and pathogenesis.

Ebola Virus Entry

A major goal of this laboratory has been to identify the host factors that mediate infection by the Ebola virus glycoprotein. Ebola virus (EboV) is a complex (-)ssRNA virus associated with fever, hypotension, severe bleeding and capillary leakage, and is highly fatal in humans, with a mortality of greater than 50% within 21 days of infection (Feldmann & Geisbert, 2010). Two genera of filoviruses are known, Marburg and Ebola, and of the latter there are five known species: Zaire (ZEBOV), Sudan (SEBOV), Reston (REBOV), Côte d'Ivoire (CIEBOV) and Bundibugyo (BDEBOV) (Hensley et al., 2010). The virus has a filamentous structure of up to 1.4 μm, though the diameter remains consistent at approximately 80nm (Feldman & Klenk, 1996). The virion often curls in the shape of a U or a 6 (Figure 9).

Like influenza HA and other class I fusion proteins, EboV GP is a trimer of dimers composed of transmembrane subunit GP2 and membrane distal subunit GP1 (Figure 6, far left). The structure of pre-fusion GP has been solved and contains the characteristic 3-stranded coiled coil (Lee et al., 2008). The fusion peptide is composed of a loop that wraps around the outside of

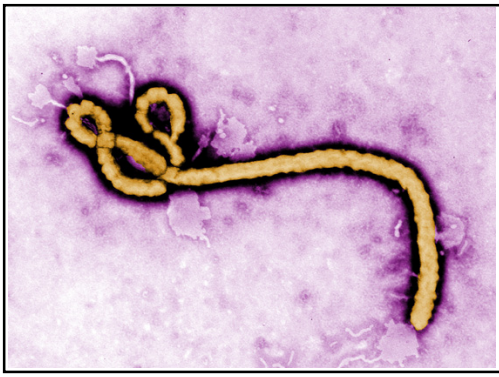

Figure 9: Electron micrograph image of the Ebola virus (Murphy, 2010).

the adjacent subunit in the trimer. The top of GP1 contains a heavily glycosylated "cap" (Figure 10, tan domain) that covers a domain associated with receptor binding and stabilization of GP1 (Figure 10, gray domain) (Lee et al., 2008). Moreover, the structure of post-fusion GP2 contains the characteristic hairpin and six-stranded helical bundle (Chen et al., 1998).

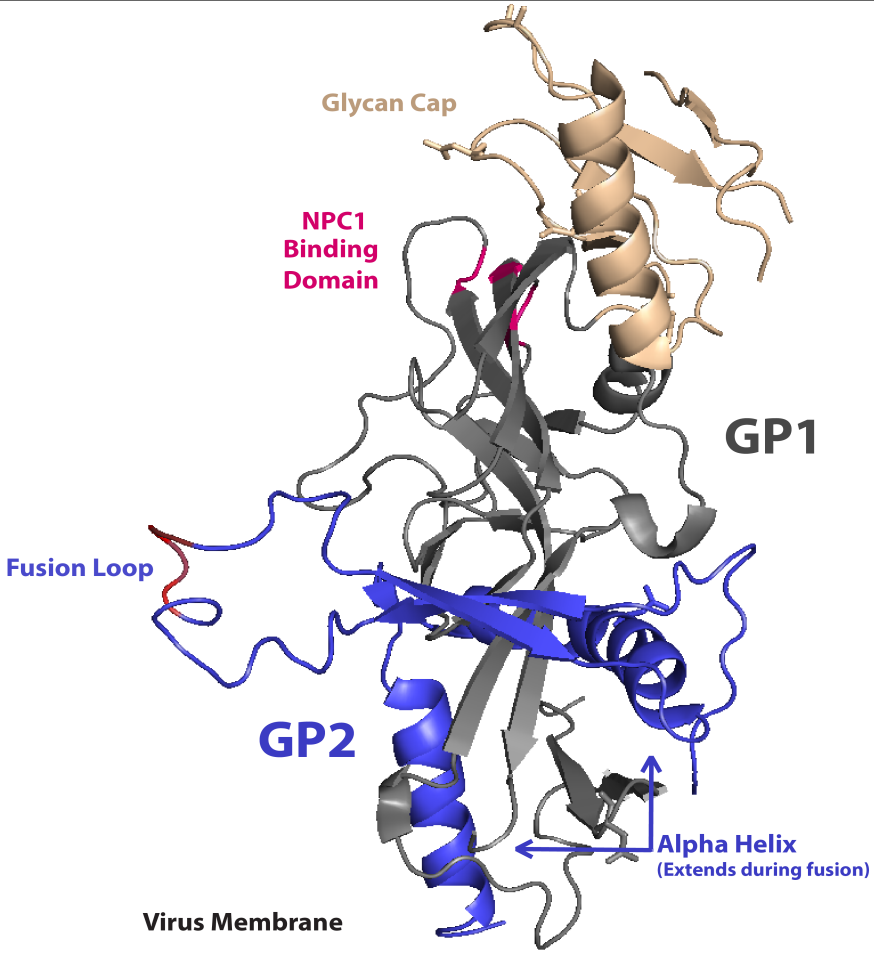

Figure 10: Location of the fusion loop in Ebola GP monomer. GP2 is highlighted in blue, with the fusion loop designated on the left and the alpha helices that comprise the coiled coil of the trimer on the lower right. The red segment corresponds to the specific residues of the loop that are focused upon in this paper. The remainder of the domains–gray, tan, and pink–comprise GP1. The tan-colored domain is the glycan cap, which is removed by cathepsin cleavage to expose the NPC1 binding domain beneath it, highlighted here in pink.

Recent studies have identified strong candidates for the host factors that trigger EboV infection. Studies show EboV particles attach to cell surface lectins and are taken up by membrane proteins that transports cholesterol into cells. This laboratory has shown that Ebola virus cannot infect cells lacking either endosomal protease cathepsin B or cholesterol transport protein NPC1. Upon incubation of EboV GP-bearing virus particles with cathepsin proteases, the glycan cap of GP1 (CHO) is removed and the virus particles are still infectious and dependent on NPC1. Moreover, the domain that binds to NPC1 (RBD) is in close contact with the domain that forms close, and likely stabilizing, contacts with GP2. A model of the function of cathepsin proteases and NPC1 in EboV GP-mediated infection has been proposed (Figure 11). At present, the role of each step in inducing the conformation changes in GP2 that are required for infection is unknown. In one scheme, cathepsin cleavage may be sufficient for release of the fusion loop of GP2 and formation of the extended conformation—thus suggesting that NPC1 binding may induce hairpin bundle formation. Alternatively, cathepsin cleavage may serve only to permit binding of NPC1, which is the trigger for both of the critical changes in GP2 conformation required for infection. To address this issue, assays are being developed to monitor membrane insertion of the fusion loop and the formation of the helical bundle. A key part of this line of investigation is to include studies of selected mutant GPs which are blocked at each step of the conformational changes in GP2. The goal of my research is to identify a mutant GP that is defective in insertion of the fusion loop of GP2 into target membranes. My hypothesis is that specific amino acids at the tip of this fusion loop of GP2 are essential for membrane insertion.

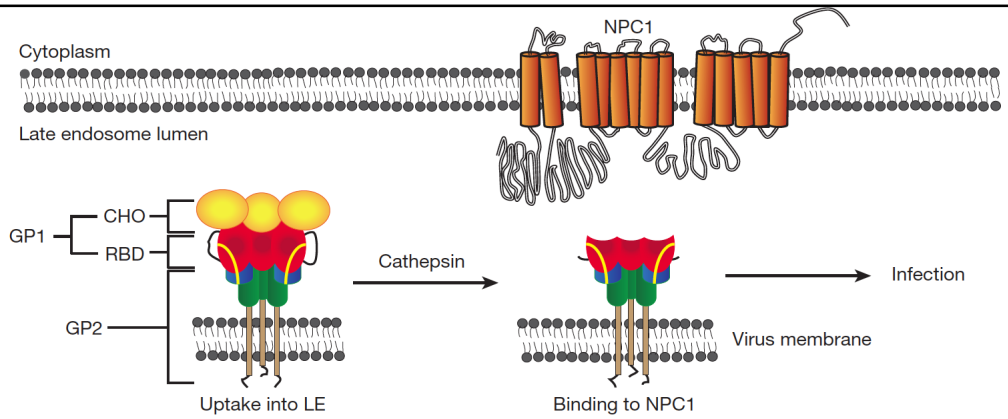

Figure 11: Proposed model of Ebola GP-facilitated membrane fusion and entry into the cell (Côté et al., 2011). After uptake via macropinocytosis and transport to endosomes, Ebola GP is cleaved by cathepsin proteases to expose the receptor binding domain (RBD), which is a ligand for NPC1. It is proposed that binding to NPC1 is the trigger for membrane fusion.

Chapter II

Materials and Methods

Site-Directed Mutagenesis

PCR site-directed mutagenesis of the GP2 fusion peptide was utilized to generate multiple GP2 mutants. Primers were generated containing single codon alterations within the fusion loop. The forward and reverse mutagenic primers were then separately combined with GP-containing plasmids and corresponding reverse and forward primers designed to anneal to sites outside the fusion peptide genome. They were amplified through PCR, generating single overlapping strands containing the mutation. The resultant products were purified through gel purification with a Qiagen DNA purification kit, then combined with the two mutagenic primers and the PCR was repeated to generate complete double-stranded mutant DNA. The DNA product was then digested at two sites outside the GP2 sequence for twelve hours, utilizing NsiI and BglII restriction endonucleases. The same digestion was performed on the intended vector for transformation, pCAGGS, followed by dephosphorylation with antarctic phosphatase for one hour. The digested DNA product and pCAGGS vector were subsequently gel purified and then ligated to one another with T4 ligase overnight.

The ligated GP mutant vector – containing a gene to confer resistance to ampicillin – was purified and then applied to high competency bacteria for transformation. The bacteria were plated and grown overnight on ampicillin-positive plates, and the resultant colonies were picked and expanded. A small sample of each colony was also taken, amplified through PCR, cut with

restriction enzymes, and evaluated on a Northern blot to ensure the full length of DNA was successfully incorporated during transformation. The bacteria was grown in broth overnight, spun down, and finally purified with a Qiagen DNA purification kit. Samples of the purified DNA were then sequenced to confirm the successful production of plasmids containing the desired mutations.

MLV Retrovirus and VLP Production

Wild type and mutant MLV retrovirus particles and virus like particles (VLPs) were produced through transfection of GP-envelope-containing pCAGGS expression vector with gag-pol in 293T cells. Mutant GP, the expression vector, and lacZ reporter gene or GFP tag gene were mixed with 10% calcium phosphate, and the mixture was added dropwise to hepes-buffered saline while vortexing. The resultant mixture was incubated at room temperature for five minutes, and then added to media over 293T cells. The cells were allowed to incubate over night, and the virus product was harvested on days two and three. The virus product was then purified through ultracentrifugation and resuspended in 250µl of buffer containing NaCl and Tris. The 293T cells were lysed through purification and resuspension in lysis buffer and the lysate isolated.

VSV Production

293T cells were plated and incubated overnight until 85-90% confluent. The GP-envelope-containing pCAGGS expression vector was mixed with 4% lipofectamine 2000 in Opti-MEM® reduced serum media and allowed to incubate for twenty minutes. The mixture was then applied drop-wise onto the cells and allowed to incubate at 37°C overnight. The following

day the mixture was removed and the media changed. On day three VSV virus was thawed and mixed in a 1:1 dilution with media, and the virus was gently applied to the cells and incubated at 37°C for one hour. The virus was then removed, the cells washed with cold media, and the cells were incubated again for 48 hours. On day five the media was removed, purified through ultracentrifugation, and resuspended in 250µl buffer containing NaCl and Tris.

Membrane Purification

NPC1-overexpressing cells and NPC1-negative cells were grown in 15cm dishes until confluent. The cells were then washed with PBS and resuspended in a 0.25M sucrose solution containing 10mM Na_2EDTA and100mM HEPES. The cells were lysed in a douncer, spun down at 1,500g for ten minutes, and the supernatant isolated. This step was repeated once more and the isolated supernatant was then spun down at 15,000g for 30 minutes at 4°C. After spinning, the supernatant was removed and the resultant pellet was resuspended in 664µl of the sucrose solution. This was then mixed with 36µl of 10% BSA and 0.2 ml of Percoll stock solution comprised of 90% Percoll and 10% of a diluent containing 2.5M sucrose, 10 mM Na_2EDTA, and 100mM HEPES. The mixture was ultracentrifuged for 30 minutes at 36,000g in a fixed angle rotor at 4°C. The resultant gradient was fractionated and a β-N-Acetylglucosaminidase assay was utilized to identify the fraction containing purified membranes.

The β-N-Acetylglucosaminidase assay was utilized to identify the gradient fractions of lysed ultricentrifuged cells containing purified membranes. For each fraction, 2µl of sample was mixed with 22.5µl of water, 48µl of a buffer containing 0.3 M citric acid, 0.3 M trisodium citrate dihydrate, and 0.3 M NaCl, and 25µl of a substrate buffer containing 1.5 mM of 4-methylumbelliferyl-N-acetyl-β-D-glucosamide. This mixture was incubated for one hour at

37°C. The consequent chemical reaction was then halted through the addition of 200µl of bicarbonate buffer containing 0.5 M sodium carbonate and 0.5 M sodium bicarbonate. The mixtures were then excited at a wavelength of 360 nm and fluorescence emission was read at 448 nm.

Thermolysin Cleavage

Virus was resuspended in NT buffer (0.5 mM NaCl, 10 mM Tris-HCl, pH 8). A 2mg/ml solution of thermolysin was combined with the virus and NT buffer solution in a ratio of 1:1:8, achieving a final thermolysin concentration of 200 µg/ml. The solution was then incubated in a 37° C water bath for 45 minutes, after which the reaction was killed by incubating it with 500 µM phosphoramodine for 10 minutes on ice.

Flow Cytometry

WT8 cells were infected with GFP-encoded MLV virus overnight, followed by a change in media. After 48 hours, the infected cells were trypsinized, washed in a washing buffer (PBS with 2% FBS), and resuspended in the same buffer. The percentage of GFP positive cells was then measured by flow cytometry using FACScalibur.

Infection Assay with MLV Retrovirus

Target cells

WT8 or Vero cells were plated in 24-well plates and allowed to incubate overnight until they were approximately 50% confluent. The following day wild type and mutant GP-containing MLV retroviruses with the LacZ reporter gene, which expresses the enzyme β-galactosidase,

were added to each well at varying concentrations. After 72 hours the cells were washed with PBS and fixed with paraformaldehyde. For the Vero cell assays, the viruses were also purified and concentrated approximately 100-fold into 250µl solutions prior to application.

Staining

Infection was detected through staining with x-gal which, when cleaved by β-galactosidase, produces a vibrant blue oxidized product. The x-gal was buffered in PBS with 2 mM MgCl2, 5 mM ferricyanide, and 5mM potassium ferrocyanide. It was then applied to the fixed cells and they were left to incubate overnight. The cell staining was evaluated the following day via microscopy.

Production of GP Trimer

Mutant GP and the expression vector with His tag and trimerization domains were mixed with 10% calcium phosphate, and the mixture was added dropwise to hepes-buffered saline while vortexing. The resultant mixture was incubated at room temperature for five minutes, and then added to media over 293T cells. The cells were allowed to incubate over night, and the virus product was harvested on days two and three.

900 µl of the supernatant was then mixed with 100 µl of pH 8 binding buffer containing 500 mM sodium phosphate, 1.5 M NaCl and 100 mM imidazole. His-tag purification magnetic beads were washed five times with pH 8 wash buffer containing 50 mM NaH_2PO_4, 300 mM NaCl, ad 20 mM imidazole. The supernatant mixture was run through beads overnight. The beads were then washed with 10x their volume of wash buffer. The trimers were eluted with

buffer containing 50 mM NaH_2PO_4, 300 mM NaCl, and 250 mM imidazole. The eluent was then dialize through a 3,500 MWCO membrane.

Co-Immunoprecipitation

Wild type and mutant GP trimers were tested for binding to NPC1 via a co-immunoprecipitation assay. The GP trimer was cleaved with thermolysine for 45 minutes in buffer containing NaCl and Tris. The trimer was then combined with a solution of purified membranes expressing NPC1 and allowed to incubate for one hour. Lysis buffer containing 10% CHAPSO was added and the membranes were permitted to lyse for 20 minutes. The mixture was then spun down at 15,000 rpm for ten minutes, and the resultant supernatant was removed and mixed with anti-NPC1 antibodies overnight at 4°C. The following day this was mixed with agarose beads suspended in CHAPSO lysis buffer and agitated in a rotator for four hours at 4°C. The beads were then spun down and washed with CHAPSO three times. They were mixed with the elution buffer, 0.1M glycine at pH 3, and allowed to incubate for five minutes. The eluent was then removed, neutralized with 1M Tris at pH 8, and combined with loading buffer for subsequent gel electrophoresis.

Fluorescent Microscopy with Virus-Like Particles (VLPs)

Vero cells were plated in 24-well plates and allowed to incubate overnight until they were approximately 50% confluent. The following day wild type and mutant GP- and GFP-expressing VLPs were added each to three wells, generating three sets of wells. The first set was fixed immediately with paraformaldehyde, the second after 45 minutes, and the third after 4 hours. The infected cells were then imaged via fluorescent microscopy.

Chapter III

Results

A major goal of this laboratory is to test the model of Ebola virus infection illustrated in Figure 11 and to correlate findings with membrane fusion by virus GP2. The focus of my research has been to identify EboV glycoproteins that are specifically defective in insertion of the fusion loop of GP2 into host cell membranes.

Strategy

The strategy to achieve this goal was derived from examination of the structure and amino acid sequence of the fusion loop (Figure 12). Based on studies of EboV GP2 and other virus membrane fusion proteins, I hypothesized that hydrophobic residues located at the very tip of the loop are likely to insert into the target membrane and thus would be strong candidates for targeting amino acid substitutions that would render them unable to enter the membrane and initiate infection. Given this, I postulated that I532, P533, Y534, and F535 are candidate residues that are essential for infection (Figure 12a).

Design of Mutants

My approach to test the role of these amino acids in infection was to introduce specific substitutions that might abrogate the membrane fusion function and test the effects on infection. To this end, I applied site-directed mutagenesis as a means to introduce the changes—I532A,

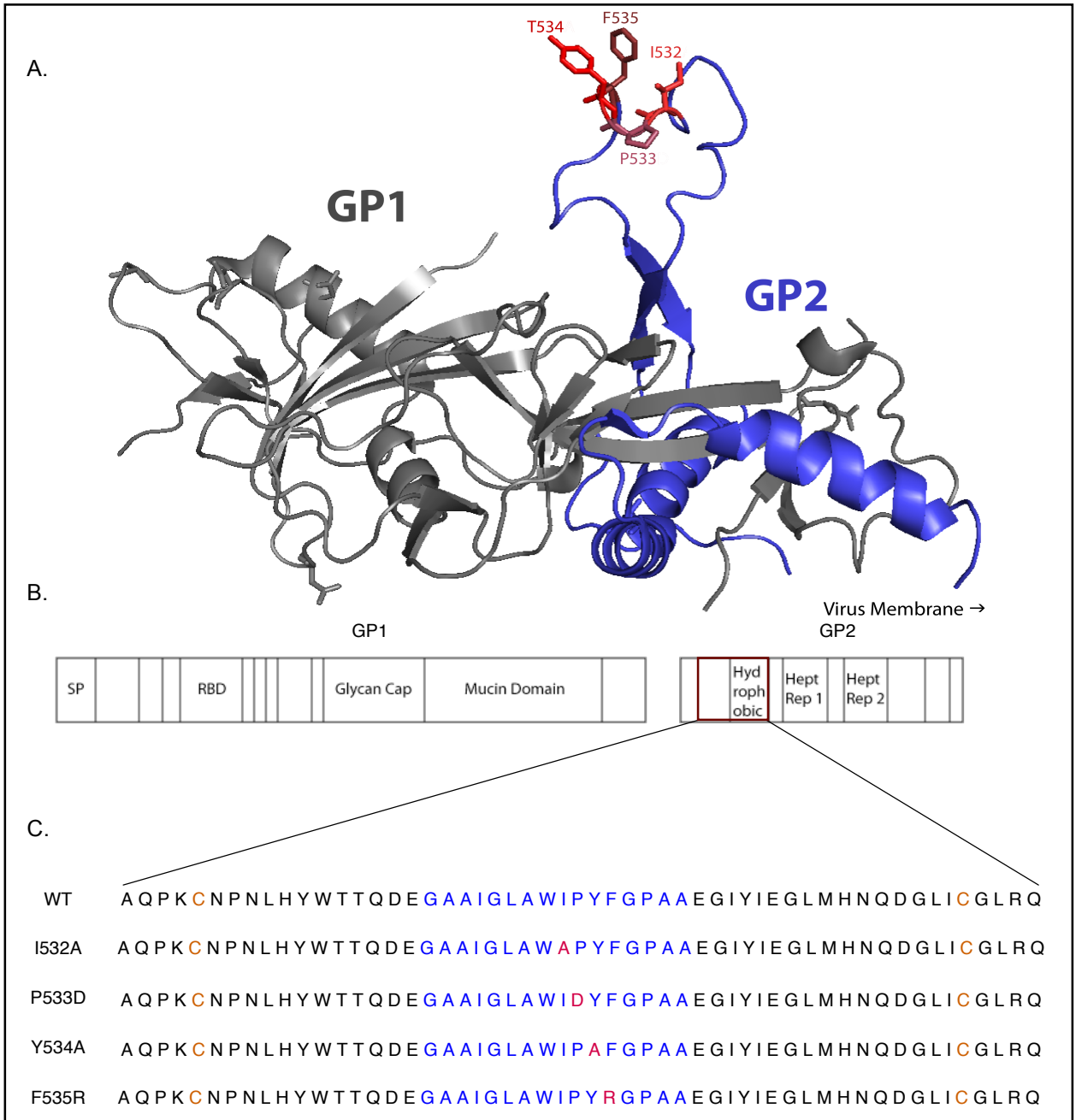

Figure 12: Selection of candidate residues in fusion loop that may be essential for membrane fusion.
A) The sites of mutagenesis are shown in the context of the fusion loop. The mutated residues are shown in red on the tip of the fusion loop. The remainder of the GP2 subunit is shown in blue and the GP1 subunit is shown in gray.
B) The position of the fusion domain (red box) within the linearized GP protein structure is depicted. The bar on the left corresponds to GP1 while that on the right corresponds to GP2. SP refers to the signal peptide, RBD to the receptor binding domain, and Hept Rep to the heptad repeats that are critical in the formation of the helical structured "spring" mechanism that releases the fusion loop into the membrane.
C) The fusion peptide sequences of each mutant are compared to that of the wild type (WT). Each amino acid mutation is designated in red.

P533D, Y534A, and F535R—into a pCAGGS expression plasmid encoding EboV Zaire GP (Figure 12c). I designed oligonucleotide primers with single-codon alterations to generate overlapping strands of DNA via PCR that, when combined in a subsequent PCR, generate a double stranded DNA segment containing the mutation. I then digested this segment with NsiI and BglII restriction endonucleases and ligated the product into unidirectionally into pCAGGS mammalian expression plasmid. To confirm correct the structure of these plasmids, I used restriction enzyme mapping and nucleic acid sequencing. After the presence of the sequences encoding the amino acid substitutions were confirmed, I used these mutant plasmids to generate recombinant viruses that expressed the mutant GPs and tested them for infection. Since the experiments using Ebola virus must be performed under restrictive BL-4 safety conditions, the analysis of EboV GP was performed using murine retroviruses and vesicular stomatitis virus particles in which the native glycoprotein has been removed and replaced with Ebola virus GP (pseudotyping) (Takada et al., 1997; Wool-Lewis et al., 1998; Chandran et al., 2005; Schornberg et al., 2006; Côté et al., 2011). Previous studies indicate the entry of these virus particles into cells utilizes the same host factors as wild type filoviruses (Chan et al., 2001).

I transfected the mutant GP with MLV structural proteins *gag* and *pol* and a retroviral vector containing the gene *LacZ* between long term repeat (LTR) promoters. This produced a pseudotyped MLV virus containing the mutant GP and encoding marker lacZ. *LacZ* gene expresses β-galactosidase, the production of which permits detection of infected cells expressing lacZ using the colorimetric lacZ substrate compound x-gal (5-bromo-4-chloro-indolyl-β-D-galactopyranoside). In some experiments, I used a vector encoding green fluorescent protein (GFP) and identified infected cells by flow cytometry.

Experiments were performed to determine if the amino acid substitution in the fusion loop impaired infection but not other essential properties of GP including folding, furin cleavage, incorporation into virus particles, sensitivity to cathpesin cleavage and binding to NPC1.

Effect of Amino Acid Substitutions in Fusion Loop on Assembly and Virus Incorporation of GP

To assess the effect of substitutions on GP folding and processing, immunoblots of the purified virus and the lysates of the transfected cells were performed utilizing an anti-GP1 antibody as the probe (Figure 13). Comparing the amount of GP on the surface of the virus to the amount of GP being produced within the cells allowed me determine whether the mutant and wild type GPs were being incorporated onto the surface of the virus with similar efficiency. The results demonstrate that a 70kDa band that identified by the anti-GP1 antibody is present in equal amounts in native and mutant GPs (Figure 13). These findings indicate the presence of the substitutions in the fusion loop do not alter the processing or incorporation of GP into virus particles.

Effect of Amino Acid Substitutions on Virus Infectivity

Once incorporation of the GPs into the MLV virions was confirmed, I measured infection using two assays. In one assay, the target cells are Chinese hamster ovary cell line WT8 expressing human NPC1. WT8 cells were exposed to MLV particles encoding GFP and pseudotyped with native or mutant GPs and infection was assessed using flow cytometry (Figure 14). The results show that the presence of the substitutions in GP2 markedly reduced infection. The mutant GP I532A and Y534A were reduced by 90% and P533D and F535R were reduced by

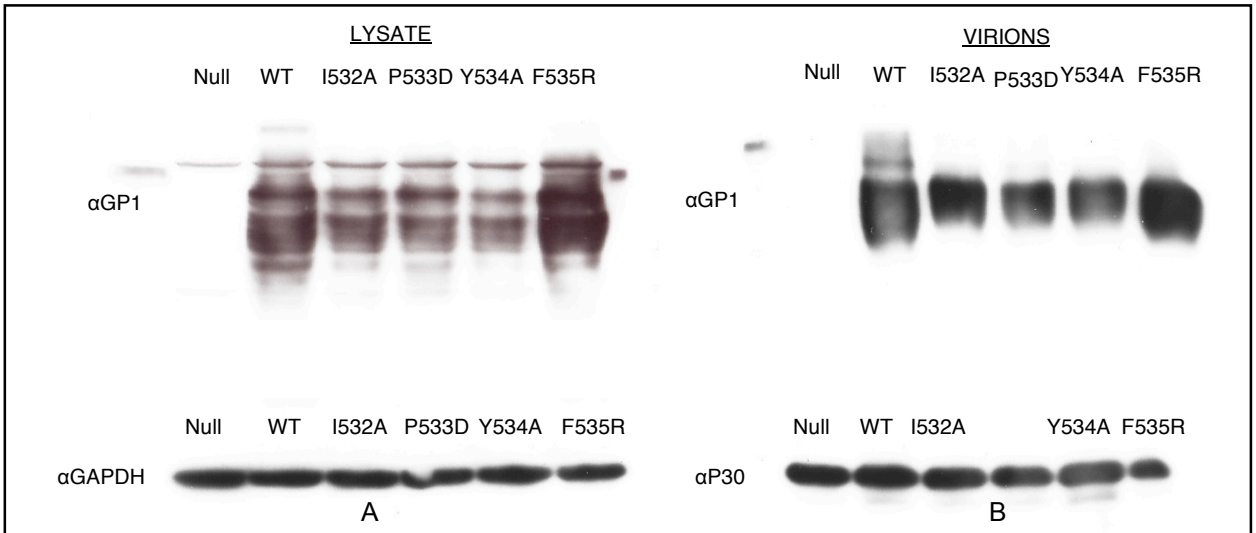

Figure 13: Expression and virus incorporation of mutant glycoproteins. A) Western blot of 293T lysate with αGP1 antibody illustrates glycoprotein production within transfected cells. The housekeeping protein GAPDH was utilized as a loading control B) Western blot of the virus particles with αGP1 antibody shows incorporation of GP at levels that correspond to protein production in transfected cells. P30, the capsid protein of MLV, was utilized as a control for the amount of viral particles.

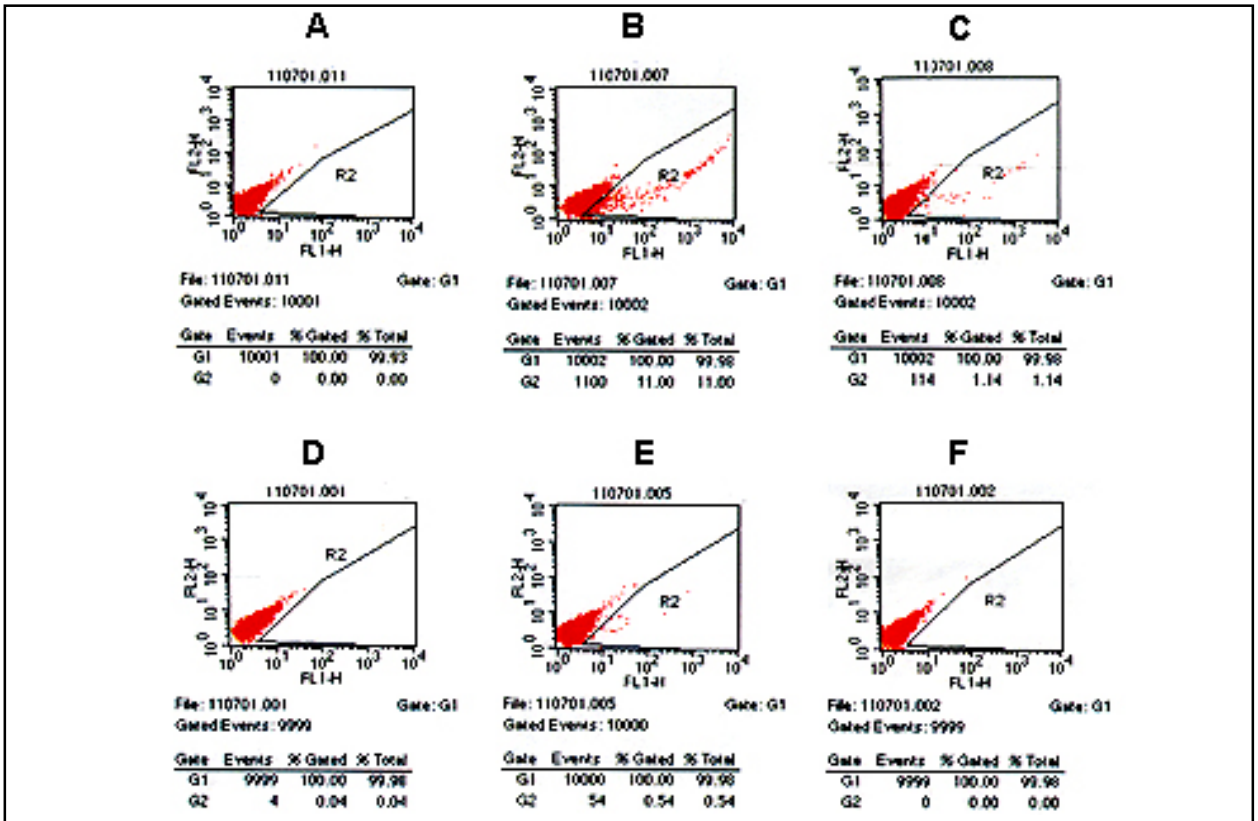

Figure 14: Infectivity of VSV expressing mutant GP. Flow cytometry was utilized to measure the expression of GFP in Vero cells, an indicator of successful infection by GFP-encoded viruses. **(**A) Negative control (B) WT GP (C) GP I532A (D) GP P533D (E) GP Y534A (F) GP F535R

>99%. Coupled with the studies of GP processing, these results indicate that amino acids I532, P533, Y534, and F535 are important for infection.

To confirm this finding, the experiment was repeated using an MLV vector encoding β-galactosidase that permitted more sensitive quantitation. The relative infection by each virus was compared to virus expressing the unaltered wt GP (Table 3). The experiment was also repeated in Vero cells, which are even more sensitive to EboV infection (Table 4). The findings confirm the initial results using WT8 cells and show that GP I532A infection is 10% of virus particles expressing wild type (WT) GP, GP Y534A is 1% of WT, and neither P533D nor F535R supported any detectable infection under conditions where the titer of the WT virus exceeds 10^5 infectious units/ml. Thus, both P533D and F535R have a profound effect on EboV GP-dependent infection.

Focus-Forming Units / ml	
GP2	**Batch 1**
Wild Type	3.18 x 10^4
I532A	2.06 x 10^3
P533D	<10
Y534A	5.25 x 10^2
F535R	<10

Table 3: Infectivity of MLV expressing mutant GP in WT8 cells. Infection rates were determined via LacZ staining of infected cells followed by counting of focus-forming units.

Focus-Forming Units/ml		
GP2	**Batch 2**	**Batch 3**
Null	<10	<10
Wild Type	2.45 x 10^5	2.79 x 10^5
I532A	6.71 x 10^4	2.98 x 10^4
P533D	<10	<10
Y534A	2.61 x 10^3	2.20 x 10^3
F535R	<10	<10

Table 4: Infectivity of MLV expressing mutant GP in Vero cells. Infection rates were determined via LacZ staining of infected cells followed by counting of focus-forming units.

Effect of Amino Acid Substitutions on Host Factor Interactions

After demonstrating the effects of the GP2 substitutions on virus infectivity, I sought to determine the stage of the viral entry pathway that was impeded. While the substitutions, as suggested by their location, were designed to specifically target the insertion of the GP2 helix trimer into the membrane, the possibility remained that these substitutions might also alter other functions of GP requisite to trigger fusion.

Two factors that are known to be required to trigger fusion in Ebola GP are cathepsin cleavage and binding to NPC1 (see Figure 11) (Chandran et al., 2005; Schornberg et al., 2006; Côté et al., 2011). To test the first, I studied infection by virus particles that were cleaved with the metalloprotease thermolysin. Thermolysin is a thermostable zinc metalloproteinase that has been shown to cleave GP1 from 35 kDa to 17kDa, which faithfully mimics the action of lysosomal cathepsins (Schornberg et al., 2006; Côté et al., 2011). After incubation of virus particles for 30 minutes in thermolysin, the cleavage of GP1 was analyzed by immunoblot (Figure 15). The cleavage of GP1 from F535R and I532A GPs was identical to wt GP. However, thermolysin only partially cleaved Y534A and P533D was completely degraded. This protocol was repeated using limited cleavage (Figure 16) and demonstrated that GP P533D is rapidly degraded and cleavage of GP Y534A is altered as evidenced by formation of an unexpected intermediate that is completely degraded over time. In addition, the findings show that the rate of cleavage of I532A but not F535R is slowed compared to WT. Thus, these findings indicate that changes in the fusion loop of GP2 do effect sensitivity to cleavage of GP1.

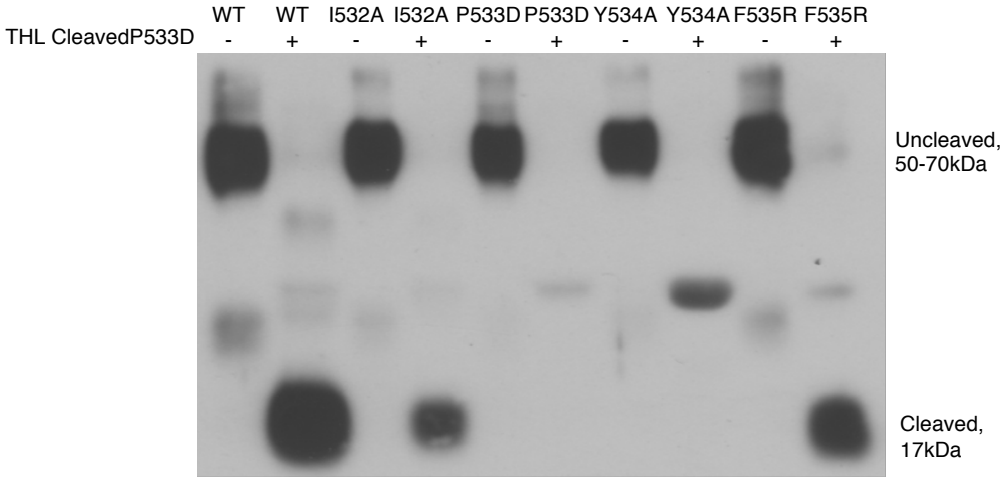

Figure 15: : Effect of substitutions in GP2 fusion loop on proteolytic cleavage of GP1. GP was expressed on the surface of MLV. Uncleaved protein is indicated by the 50-70kDa bands, while the fully cleaved protein is distinguishable at approximately 17kDa. Mutants 1532A and F535R generate cleavage products similar to WT.

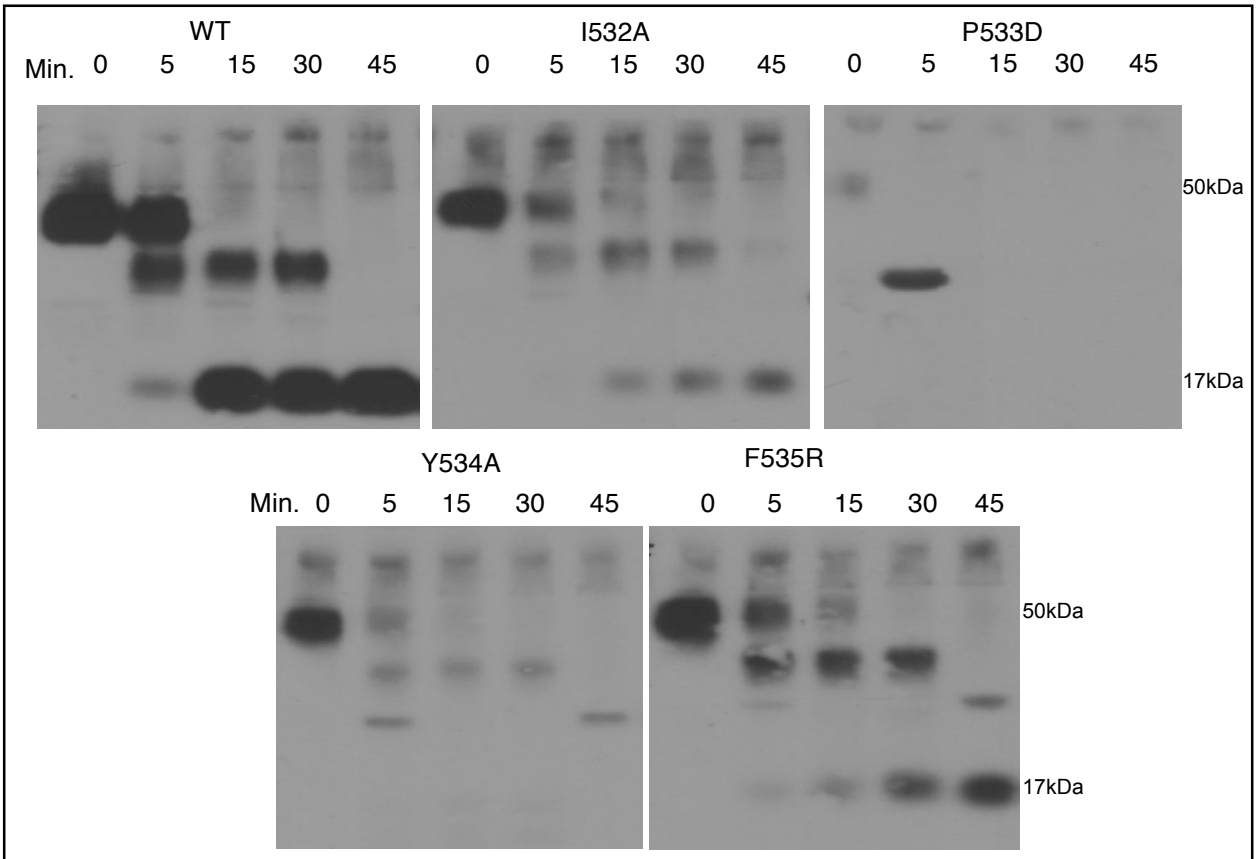

Figure 16: Further analysis of the effects of amino acid substitutions on GP cleavage. Wild type and mutant GP were cleaved by thermolysin over the course of 45 minutes. The reaction was halted at specific time intervals and the cleavage product was evaluated via western blot for GP. Uncleaved protein is indicated by the 50-70kDa bands, while the fully cleaved protein is distinguishable at approximately 17kDa.

However, the substitution of F535R does not alter processing, incorporation, stability or proteolytic cleavage of GP1 but completely abrogates GP-mediated infection.

To further assess the function of GP F535R, binding studies using NPC1 as target were performed. The approach was to use a co-immunoprecipitation assay developed in our laboratory (Côté et al., 2011). Virus particles were incubated in thermolysin to cleave GP1 and then further incubated with intracellular membranes from cells expressing or lacking NPC1. After incubation to allow binding of cleaved GP1 to NPC1, NPC1 was precipitated using anti-NPC1 antibody and recovered using Protein A beads that bind to Ig. These beads were washed and then bound proteins were eluted by boiling and analyzed by immunoblot. I found that both WT and mutant F535R GP were specifically recovered on beads containing NPC1 antibody (Figure 17). These findings demonstrate that the F535R does not interfere with binding of protease-cleaved GP1 to NPC1 receptor.

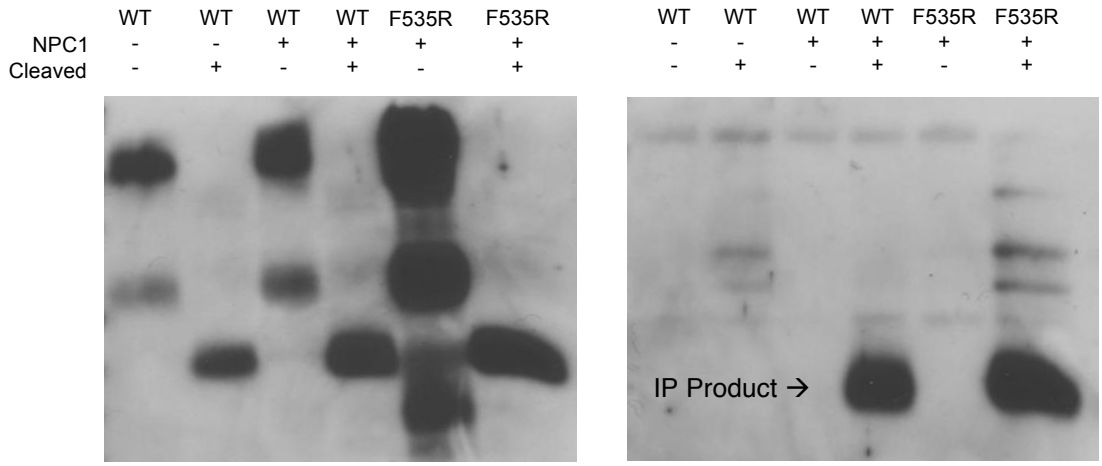

Figure 17: Effect of GP2 F535R on binding of cleaved GP1 to NPC1 receptor. F535R mutant GP was produced as a trimer and mixed with NPC1-containing membranes before solubilization in lysis buffer. Anti-NPC1 antibodies were applied and coupled to agarose beads. The beads were then washed and the co-immunoprecipitation product was eluted, followed by evaluation via western blot using anti-GP antibodies. Left: Blot of lysates. Right: Blot of co-immunnoprecipitates.

Taken together, my findings indicate that the defect in infection conferred by F535R is not caused by altered processing, cleavage or binding to NPC1 receptor.

Effect of Amino Acid Substitutions on Virus Trafficking

Finally, it was necessary to rule out the possibility that the amino acid substitutions on the GP fusion loop were altering the attachment of virus particles to cells and/or subsequent trafficking from the cell surface to intracellular late endosomes and lysosomes that contain cathepsin proteases and NPC1. To evaluate this, I incorporated I532A and F535R GPs into GFP-tagged filovirus-like particles (VLP-GFP) formed from EboV VP40 matrix protein tagged with GFP. Target cells were incubated with VLPs at 4^{o}C to promote binding to the cell surface. At intervals after warming to 37^{o}C, the location of the VLPs in the cells was assessed using fluorescence microscopy (Figure 18). Bald particles and particles incorporated with VSV-G glycoprotein served as controls. The data indicate that GPs bearing changes in GP2 are taken up into cells and trafficked to internal vesicles at the same rate and location as VLPs expressing WT GP. The localized fluorescent intensity of particles expressing WT and I532A GPs was diminished after four hours, which is indicative of fusion of the VLP membrane to host membranes. In striking contrast, the fluoresence of particles expressing GP F535R VLP-GP was not dissipated, strongly suggesting these particles were unable to fuse with target cell membranes despite successful uptake by cells and trafficking to intracellular vesicles.

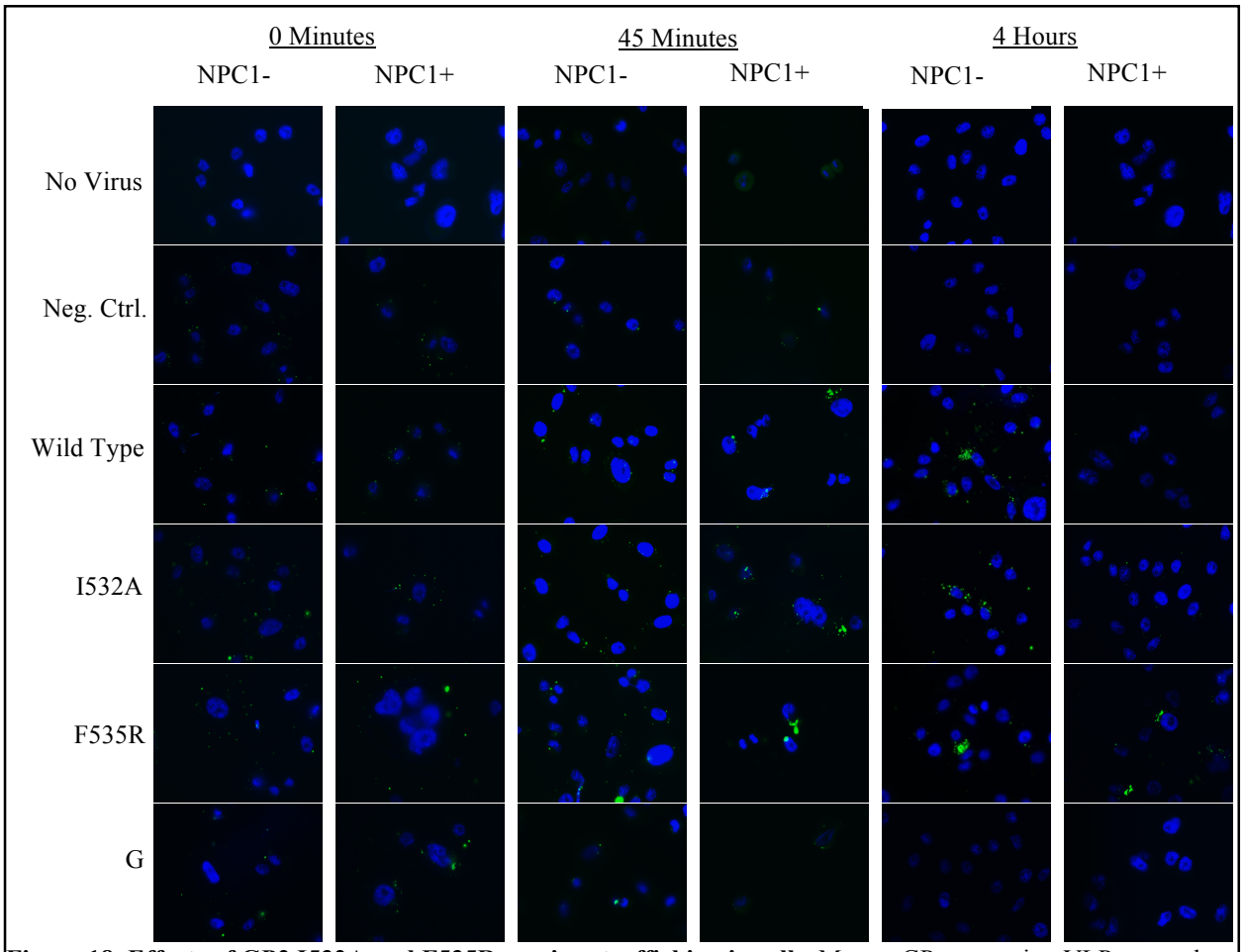

Figure 18: **Effects of GP2 I532A and F535R on virus trafficking in cells.** Mutant GP-expressing VLPs tagged with GFP were localized via fluorescence microscopy at (a) 0 minutes, (b) 45 minutes, and (c) 4-hours post-infection and compared to VLPs expressing wild type GP and VSV-G.

Chapter IV

Discussion

The goal of this study was to identify EboV GPs that are competent for assembly and interaction with host factors, but defective for infection. The principal finding is that substitution of arginine for F535 in the fusion loop meets these criteria.

Rationale of Approach and Conclusions

The strategy to generate the altered GPs first required the identification of suitable candidate residues for substitution. Previous mutational analyses of EboV and other class I viruses suggested the most promising targets resided between residues 529 and 536 of the disulfide-bonded loop that mediates membrane fusion (Ito et al., 1999; Delos, Gilbert, & White, 2000; Gregory et al., 2011). Of these, I selected residues 532, 533, 534, and 535 that have hydrophobic side chains are exposed. Alanine, the most conservative of the choices due to its hydrophobicity and small size, was selected as the replacement peptide for non-polar residues I532 and Y534. Aspartic acid was chosen to replace the proline on residue P533, introducing a negative charge that likely alters the local conformation by removing the chain-breaking proline residue necessary to maintain the loop structure. Finally, the phenylalanine of residue F535 was replaced with arginine, which has a positively-charged side chain that may be restricted in its ability to penetrate the hydrophobic environment of the target cell membrane that is required to mediate membrane fusion.

GPs carrying these amino acids substitutions GP2 were successfully processed and incorporated into the virus membrane. GP F535R showed similar levels of cell expression as wild type GP while substitutions I532A, P533D, and Y534A displayed slightly reduced expression/stability. Also, expression correlated with incorporation into virus particles, suggesting that transit through the secretory pathway is not impaired. The reduced production within the cells of these mutants may have been the result of lower transfection efficiency, however it is also possible that changes to the structure of the protein caused by the mutations led to increased misfolding of the protein or to unknown difficulties in its insertion into the membrane of the endoplasmic reticulum. Additional studies of transfection efficiency and protein trafficking are required to address this question.

After confirming successful incorporation I evaluated the mutants for infectivity, to ascertain whether any of the mutations may have resulted in a loss of GP function. In the flow cytometry assay, the level of fluorescence above background for wild type virus and the I532A and Y534A mutants showed that infection had occurred, while the absence of fluorescence for mutants P533D and F535R and the negative control virus, which contained no GP, indicated that infection had not been successful (Figure 14). The results suggested that at least two of the mutants, P533D and F535R, were non-functional. The more rigorous LacZ staining assay confirmed this. The resultant focus-forming units showed that, as compared to wild type, infectivity was reduced by approximately one log for I532A mutants, two logs for Y534A mutants, and impeded completely in the case of P533D and F535R mutants (Table 3). Repeat experiments in Vero cells provided similar results (Table 4).

An important finding from my studies was the comparison of these two methods of measuring GP-dependent infection. I found that flow cytometry of cells exposed to GFP

encoding virus was rapid but much less sensitive than the focus-forming assays based on cell expression of virus encoded lacZ. Thus, the GFP assay is suitable for screening of larger numbers of mutant proteins to identify candidates for further quantitative study using lacZ virus. The latter assay was essential to showing that F535R completely abrogated EboV GP infection. The result confirms the findings in a previous report (Ito et al., 1999) that analyzed function of EboV GP2.

While these results suggested that the substitutions in GP2 inhibited membrane fusion, the possibility remained that some other step in the entry pathway was also being affected. Thus it was necessary to test the mutant viruses for the effects of protease cleavage. A key observation was that substitutions P533D and Y534A altered cleavage of GP by thermolysin. This is consistent with the location of the fusion peptide adjacent to the exposed loop in GP1 that is the substrate for the protease. While the F535R and I532A mutants produced a product similar to that of the wild type, the Y534A mutant seemed to generate a larger intermediate while the P533D mutant disappeared entirely, suggesting that it was completely hydrolyzed (Figure 15). The absence of any uncleaved I532A product in the thermolysin-cleaved band suggested that it too may be completely hydrolyzed after passing through the observed intermediate stage. To investigate these results further a time-course experiment was utilized to assess the effects of thermolysin for each mutant at different time-points in the cleavage process (Figure 16). P533D and Y534A were found to both be degraded, though they appeared to pass through an intermediate in the process, one which remained detectable after 45 minutes in the case of Y534A. Moreover, the I532A cleavage product is much smaller than its input, suggesting that it too is partially lost to complete hydrolysis during cleavage. Only cleavage of the F535R mutant and the wild type GP appeared to result in a final product similar in quantity to the input. The

findings indicate that local changes in structure were conferred by the substitutions that affected protease sensitivity. However this is not a general property of the fusion loop since substitutions I532A and F535R did not alter the sensitivity of GP1 to the protease. Further analysis of cleavage intermediates may reveal how substitutions alter sensitivity to proteolytic cleavage.

Based on these findings, GP F535R was the most likely candidate to serve as a fusion-defective glycoprotein. However, it remained uncertain whether it would interact with NPC1, so I tested the mutants for binding interactions with this putative receptor. I clearly established that this altered GP is fully competent to bind to NPC1 (Figure 17). Though it cannot be quantitatively measured via this method, the binding affinity of the mutant and wild type appear similar given their respective inputs. Moreover, co-immunoprecipitation of GP F535R with NPC1 was achieved after successful processing by thermolysin to remove the glycan cap, providing evidence to support the proposition that, in both cases, the NPC1 binding domain is exposed through cathepsin cleavage. Further studies measuring the extent of binding of WT and mutant GPs to NPC1 membranes as a function of cleaved GP concentration are needed to determine if F535R alters the affinity of the GP1 receptor binding domain binding to NPC1. This is unlikely because the determinants of binding are located in the receptor binding domain which is at the top of GP1 and not adjacent to the GP2 fusion loop (Figure 14).

The trafficking of GP F535R particles was not altered (Figure 18). Moreover, loss of cell-associated fluorescence by VLPs was observed with wild type and I532A but not F535R GP, which after four hours continues to present a strong fluorescence signal. Indeed, the signal from the F535R virus in NPC1+ cells resembles that observed for all three viruses in NPC1- cells. This indicates that GP F535R particles can be used to determine the site of virus membrane

fusion and entry of the virus core into the cytoplasm. My prediction is that this location will correspond to the location of NPC1, which is the trigger for EboV membrane fusion.

These data suggest that GP F535R is defective because the fusion loop is unable to insert into the target cell membrane. Additional experiments to test this conclusion are planned. Specifically, virus particles will be loaded with lipophilic dyes and NPC1 binding-induced transfer of the dye to artificial membranes will be measured as an indicator of membrane fusion. The expectation is that the rate of dye transfer will be markedly impaired in F535R compared to WT GP.

Consideration of Other Substitutions in GP2

One interesting question to consider is why the other three substitutions didn't have the same properties as F535R. One possibility is that insertion of small hydrophobic alanine residue does not impair membrane fusion. A look at the local environment of these residues in GP2 reveals that they are folded tightly into a pocket of surrounding residues from both the GP1 and GP2 subunits (Figure 19). Even slight perturbations to structure or chemistry could have significant effects on correct folding. This may very well be the case for P533D substitution. The time course of thermolysin cleavage (Figure 16), indicated that the GP P533D is degraded in as little as fifteen minutes. Misfolding associated with the P533D mutation might mean that the initial cleavage activity of thermolysin exposes additional cleavage sites on the protein that are not accessible in the wild type conformation. The cleavage of these sites might then expose yet more cleavage sites, and so on. The complete degradation of the protein would then follow in a process that can be analogized to the unraveling a sweater by pulling a single thread. Such

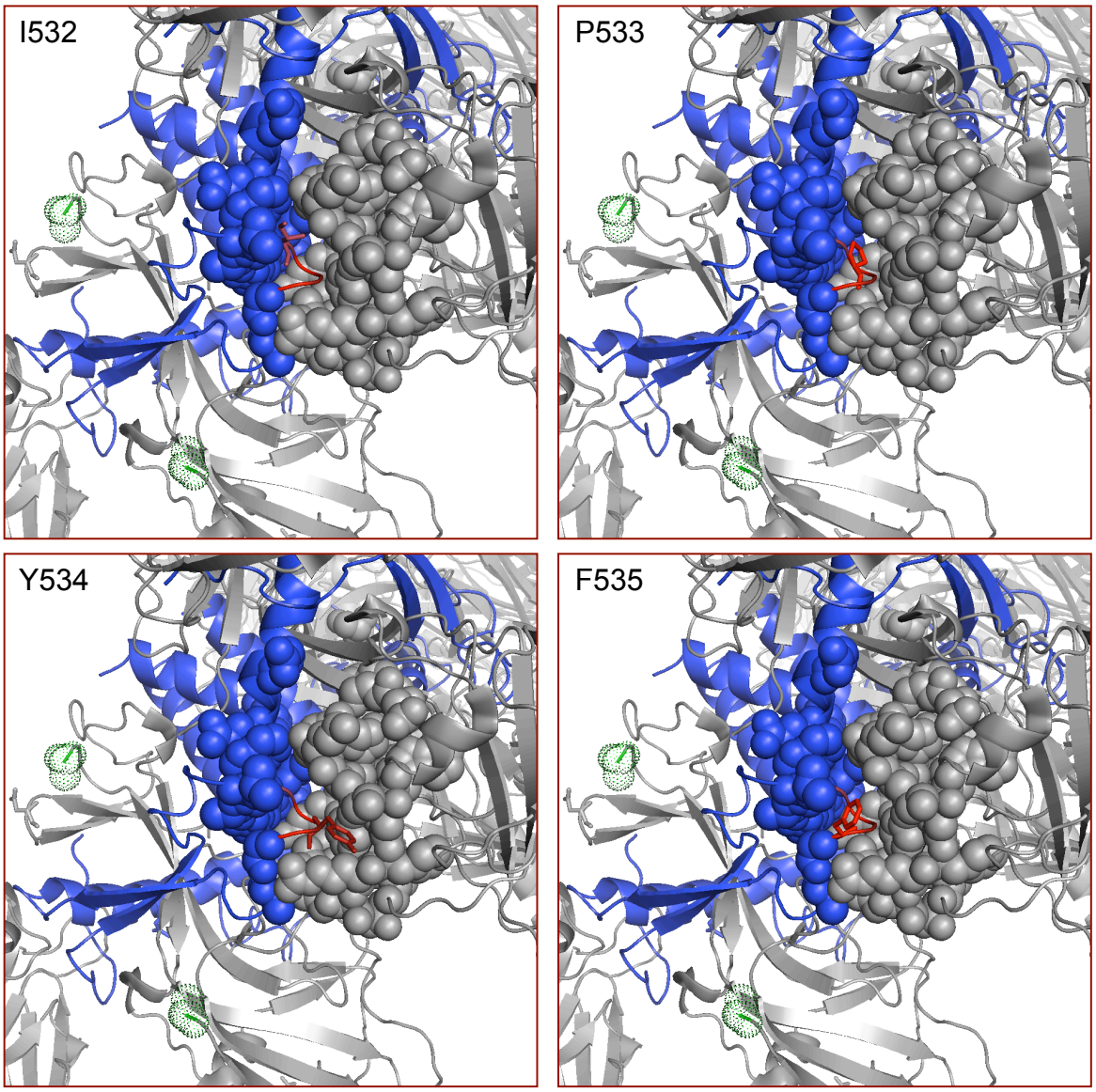

Figure 19: Residues I532, P533, Y534, and F535 of GP2 are nestled within the GP1 structure. These residues (Red) of GP2 (Blue) appear to interact closely with surrounding GP1 (Gray) residues, suggesting the effects of amino acid substitution on infectivity and cleavage may have been the result of the altered physical or chemical properties of these interactions. The loop that is targeted for proteolytic cleavage (Green, shown cleaved) passes closely to these structures.

misfolding could also be the cause of the loss of function associated with Y534A which, like P533D, demonstrates altered cleavage of GP1 by thermolysin. Disruption of secondary structures associated with P533 may also affect fusion loop function (Krieger, Moglich, &

Kiefhaber, 2005). In particular, replacement with the aspartic acid may disrupt the local structure that is required for entry into target membranes. Alternatively, the negative charge of the aspartic acid side chain may prevent insertion into target membrane with phospholipid head groups.

Future Directions

The studies reported here outline a protocol to identify, create and test the effects of amino acid substitutions in the fusion loop of Ebola virus GP2 that can be used as key reagents in future studies of how binding of GP1 triggers virus membrane fusion and infection.

Given that each residue substitution in these experiments resulted in some reduction in infectivity there is a significant likelihood that all are important with respect to infection. Though other alterations to P533 are likely to have similar outcomes, in light of its probable importance in the formation of the loop, future experiments might seek to alter the I532 and Y534 residues to arginine as well, and characterize the effects. Other residues within the loop that should be considered for arginine substitution and characterization include L529, A530, W531, G536, and P537.

Amino acid residues in the hr1/hr2 segments of GP2 that form the six-stranded helical bundle are also candidates for substitutions that disable membrane fusion and infection. This would result in viruses that could insert into the membrane but are unable to complete infection. Substitutions with these properties have been identified in influenza HA and were integral in determining the critical importance of the six-helix bundle for pore formation (Chen, Skehel, & Wiley, 1999; Eckert & Kim, 2001). Another useful non-functional mutant would be one that can be triggered even in the absence of NPC1. This would potentially allow for the isolation of

attachment from triggering, and aid in the determination of whether NPC1 is an attachment factor as well as a trigger.

One of the next critical experiments is to test whether NPC1 is indeed the trigger for the spring-loaded mechanism. With this in mind, another key assay for the study of GP's interactions with putative triggering factors will be one that tests when the fusion peptide inserts into the membrane. Liposome floatation, a method that involves the centrifugation of virus and liposomal membranes in a sucrose gradient, could potentially serve this purpose. Because virus particles contain RNA, they are sufficiently dense that they will sink to the bottom of the gradient. The comparatively less dense liposomes, however, will float to the top. Since the insertion of the fusion loop is irreversible, viruses that have been triggered should attach to the liposome membrane and travel to the top of the gradient (Smith & Cunningham, 2007). Use of this assay will be crucial to confirming that the F535R substitution fails to insert. If confirmed, F535R will serve as an important control in assays of effect of NPC1 binding on membrane fusion. One possibility that could be identified is that Y535R supports associtation of virus and target membranes, but formation of fusion pore required for infection is blocked. This would provide a reagent to investigate intermediate steps in virus entry pathway.

Chapter V

Conclusion

A key reagent to test the role of cathepsin and NPC1 in the triggering of GP fusion is a mutant virus that is blocked in the step of fusion peptide insertion or bundle formation. The goal of this project was to identify such a mutant and to characterize it to sufficiently demonstrate that it is otherwise fully functional with respect to cathepsin cleavage, NPC1-binding, and infectibility. Through tests of incorporation, infection, thermolysin cleavage, and co-immunoprecipitation with NPC1 I have shown that the Y535R mutant GP meets these criteria.

In addition to demonstrating the function of the fusion loop, this non-permissive GP mutant is also useful as a tool to further interrogate GP function. Critically, it provides researchers with a negative control that is functional in all other aspects of GP expression and function aside from membrane fusion itself.

An example of the application of this negative control is in the imaging of viral entry and trafficking within the cell. As the results of the co-localization of VLP-GPs and Vero cells suggest (Figure 18), the movement of viruses across the membrane and into the cell may be discernable based on loss of GFP signal, and differences in localization patterns between functional and non-functional viruses may help to determine how they operate. The preliminary results here indicate that while the wild type and partially functioning mutant viruses appear to have fused with their target cells, as evidenced by the lack of fluorescence, the Y535R mutant remains detectable even after four hours. Such an assay might be useful, for example, in the

determination of whether compounds intended to block viral entry work by impeding membrane fusion or, rather, by affecting uptake or endosomal trafficking.

Another example of the potential application of the F535R mutant is in its use as a control for membrane fusion assays. To test whether NPC1 binding to cleaved GP1 is sufficient to trigger membrane fusion, an assay must be developed to explicitly show when fusion has occurred. Lipophilic dyes that self-quench under high concentration conditions will fluoresce when they diffuse. When virus particles the membranes of which have been loaded with such a dye fuse with their host targets, their membranes merge and the dye molecules spread across the much larger surface area. The consequent dequenching can then be detected through fluorescent spectrophotometry. The non-functional Y535R mutant will be a critical to this experiment by serving as a negative control for fusion peptide insertion or six-helix bundle formation.

References

Ahlquist, M. (2002). RNA-dependent RNA polymerases, viruses, and RNA silencing. Science, 296, 1270-1273.

Anderson, R.G. (1998). The caveolae membrane system. *Annu. Rev. Biochem. 67*, 199–225.

Backovic, M., Jardetzky, T. (2009). Class III viral membrane fusion proteins. *Curr. Opin. Struct. Biol., 19*(2), 189-196.

Ball, L.A. (2006). Virus replication strategies. In D.M. Knipe and P.M. Howley, (Eds.) Fields Virology Fourth Edition, Philadelphia: Lippincott Williams & Wilkins, pp. 119-140

Baltimore, D. (1971). Expression of animal virus genomes. *Bacteriological Rev., 35*(3), 235-241.

Bannert, N., Fiebig, U., Hohn, O. (2010). Retroviral particles, proteins, and genomes. In R. Kurth & N. Bannert (Eds.) Retroviruses: Molecular Biology, Genomics, and Pathogenesis. Norfolk, UK: Caister Academic Press.

Bergelson, L.D., Bukrinskaya, A.G., Shaposhnikova, G.I., Kacharov, A.L., Schvechenko, V.P., Kornilaeva, G.V., Fomina-Ageeva, E.V. (1982). Role of gangliosides in reception of influenza virus. *Eur. J. Biochem. 128*(2-3), 467-474.

Berger, E., Murphy, P.M., Farber, J.M. (1999). Chemokine receptors as HIV-1 coreceptors: Roles in viral entry, tropism, and disease. *Annu. Rev. Immunol., 17*, 657-700.

Bullough, P.A., Hughson.. F.M., Skehel, J.J., Wiley, D.C. (1994). Structure of influenza haemagglutinin at the pH of membrane fusion. *Nature, 371*, 37–43.

Butel, J.S. (2010). Poxviruses. In Brooks, G.F., Carroll, K.C., Butel, J.S., Morse, S.A., Mietzner, T.A. (Ed.) Jawetz, Melnick, & Adelberg's Medical Microbiology, 25th Edition. New York: The McGraw-Hill Companies.

Carette, J.E., Raaben, M., Wong, A.C., Herbert, A.S., Obernosterer, G., Mulherkar, N., Kuehne, A.I., Kranzusch, P.J., Griffin, A.M., Ruthel, G., Dal Cin, P., Dye, J.M., Whelan, S.P., Chandran, K., Brummelkamp, T.R. (2011). Ebola virus entry requires the cholesterol transporter Niemann-Pick C1. *Nature, 477*(7364), 340-343.

Carr, C.M., Kim, P.S. (1993). A spring-loaded mechanism for the conformational change of influenza hemagglutinin. *Cell, 73*, 823-832.

Carr, C.M., Chaudhry, C., Kim, P.S. (1997). Influenza hemagglutinin is spring-loaded by a metastable native conformation. *Proc. Natl. Acad. Sci. USA, 94*(26), 14306-14313.

Chan, S. Y., Empig, C. J., Welte, F. J., Speck, R. F., Schmaljohn, A., Kreisberg, J. F., Goldsmith, M. A. (2001). Folate Receptor-a is a cofactor for cellular entry by Marburg and Ebola viruses. *Cell, 106*(1), 117-126.

Chandran, K., Sullivan, N.J., Felbor, U., Whelan, S.P. & Cunningham, J.M. (2005) Endosomal proteolysis of the Ebola virus glycoprotein is necessary for infection. *Science 308*, 1643-1645.

Chen, J., Lee, K.H., Steinhauer, D.A., Stevens, D.J., Skehel, J.J., Wiley, D.C. (1998). Structure of the hemagglutinin precursor cleavage site, a determinant of influenza pathogenicity and the origin of the labile conformation. *Cell, 95*(3), 409-417.

Collier, L., Balows, A., Sussman, M. (Eds.) (1998). Topley & Wilson's Microbiology and Microbial Infections, 9th ed., vol. 4. New York: John Wiley & Sons, Inc.

Cosset, F-L., Lavillette, D. (2011). Cell entry of enveloped viruses. *Advances in Genetics, 73, 121-183.*

Côté, M., Misasi, J., Ren, T., Bruchez, A., Lee, K., Filone, C.M., Hensley, L., Li, Q., Ory, D. Chandran, K., Cunningham, J. (2011). Small molecule inhibitors reveal Niemann-Pick C1 is essential for Ebola virus infection. *Nature, 477*(7364), 344-348.

Cureton, D.K., Massol, R.H., Saffarian, S., Kirchhausen, T.L., Whelan, S.P.J. (2009). Vesicular stomatitis virus enters cells through vesicles incompletely coated with clathrin that depend upon actin for internalization. *PLoS Pathog., 5*(4), e1000394.

Daniels, R. S., Downie. J. C., Hay, A. J., Knossow, M., Skehel, J. J., Wang, M. L., and Wiley, D. C. (1985). Fusion mutants of the influenza virus hemagglutinin glycoprotein. *Cell, 40*, 431-439.

Delos, S.E., Gilbert, J.M., White, J.M. (2000). The central proline of an internal viral fusion peptide serves two important roles. J. Virol., 74(4), 1686-1693.

Doherty, G.J., McMahon, H.T. (2009). Mechanisms of endocytosis. *Annu. Rev. Biochem, 78*(31), 31.1-31.46.

Doms, R., Helenius, A., White, J. (1985). Membrane fusion activity of the influenza virus hemagglutinin, *J. Biol. Chem. 260*(5), 2973-2981

Dragic, T., Litwin, V., Allaway, G.P., Martin, S.R., Huang, Y., Nagashima, K.A., Cayanan, C., Maddon, P.J., Koup, R.A., Moore, J.P., Paxton, W.A. (1996) HIV-1 entry into CD4+ cells is mediated by the chemokine receptor CC-CKR-5. *Nature, 389*(6584), 667-673.

Düzgüneş, N., Gambale, F. (1988). Membrane action of synthetic N-terminal peptides of influenza virus hemagglutinin and its mutants. *FEBS Lett., 227*(2), 110-114.

Earp., L.J., Delos, S.E., Park, H.E., White, J.M. (2005). The many mechanisms of viral membrane fusion proteins. In M. Marsh (Ed.) Membrane trafficking in viral replication. New York: Springer-Verlag.

Eckert, D.M., Kim, P.S. (2001). Mechanisms of viral membrane fusion and its inhibition, *Annu. Rev. Biochem., 70*, 777-810

Eisen, M.B., Sabesan, S., Skehel, J.J., Wiley, D.C. (1997). Binding of the influenza A virus to cell-surface receptors: structures of five hemagglutinin-sialyloligosaccharide complexes determined by X-ray crystallography. *Virology, 232*, 19–31

Ewers, H., Romer, W., Smith, A.E., Bacia, K., Dimitrieff, S., Chai, W., Mancini, R., Kartenceck, J., Chambon, V., Berland, L., Oppenheim, A., Schwarzmann, G., Feizi, T., Schwille, P., Sens, P., Helenius, A., Johannes, L. (2010). GM1 structure determines SV40-induced membrane invagination and infection. *Nat. Cell. Biol, 12*(1), 11-18.

Feldmann, H., Geisbert, T. (2010). Ebola haemorrhagic fever. *The Lancet, 377*(9768), 849-862.

Feng, Y., Broder, C.C., Kennedy, P.E., Berger, E.A. (1996). HIV-1 entry cofactor: functional cDNA cloning of a seven-transmembrane, G protein-coupled receptor. *Science, 272*(5263), 872-877.

Flint, S.J., Enquist, L.W., Racaniello, V.R., Skalka, A.M. (2009). Principles of Virology, Third Edition. Volume II: Pathogenesis. Washington, D.C.: ASM Press

Fotin, A., Cheng, Y., Sliz, P., Grigorieff, N., Harrison, S., Kirchhausen, T., Walz, T. (2004). Molecular model for a complete clathrin lattice from electron cryomicroscopy. *Nature, 432,* 573-579.

Gallo, S.A., Finnegan, C.M., Viard, M., Raviv, Y, Dimitrov, A., Rawat, S., Puri, A. Durell, S., Blumenthal, R. (2003). The HIV Env-mediated fusion reaction. *Biochim. Biophys. Acta., 1614*(1), 36-50.

Gething, M.J., Dams, R. W., York, D., and White, J. (1986). Studies on the mechanism of membrane fusion: site specific mutagenesis of the hemagglutinin of influenza virus. *J. Cell Biol., 702*, 11-23.

Gottschalk, A. (1959). Chemistry of virus receptors. In *The Viruses*, ed. FVM Burnet, WVM Stanley, 3:51–61. New York: Academic

Gregory, S.M., Harada, E., Liang, B., Delos, S.E., White, J.M., Tamm, L.K. (2011). Structure and function of the complete internal fusion loop from Ebolavirus glycoprotein 2. *Proc. Natl. Acad. Sci. USA, 108*(27), 11211-11216.

Harrison, S.C. (2008). Viral membrane fusion. *Nat. Struct. Mol. Biol., 15*(7), 690-698.

Helenius, A. (2006). Virus entry and uncoating. In D.M. Knipe and P.M. Howley, (Eds.) Fields Virology Fourth Edition, Philadelphia: Lippincott Williams & Wilkins, pp. 99–118

Hensley, L.E., Mulangu, S., Asiedu, C., Johnson, J., Honko, A.N., et al. (2010). Demonstration of Cross-Protective Vaccine Immunity against an Emerging Pathogenic Ebolavirus Species. PLoS Pathog 6(5), e1000904.

Huang, R.T., Rott, R., Klenk, H.D. (1981). Influenza viruses cause hemolysis and fusion of cells. *Virology, 110*(1), 243-247.

Hulo, C,. de Castro, E., Masson, P., Bougueleret, L., Bairoch, A., Xenarios, I., Le Mercier, P. (2011). ViralZone: a knowledge resource to understand virus diversity. *Nucleic Acids Res, 39*(Database issue), D576-D582.

Hunter, E. (2006). Virus assembly. In D.M. Knipe and P.M. Howley, (Eds.) Fields Virology Fourth Edition, Philadelphia: Lippincott Williams & Wilkins, pp. 142–164

Ito, H., Watanabe, S., Sanchez, A., Whitt, M.A., Kawaoka, Y. (1999). Mutational analysis of the putative fusion domain of Ebola virus glycoprotein. *J. Virol., 73*(10), 8907-8912.

Kelm, S., Paulson, J.C., Rose, U., Brossmer, R., Schmid, W., Bandgar, B.P., Schreiner, E., Hartmann, M., Zbiral, E. (1992). Use of sialic acid analogues to define functional groups involved in binding to the influenza virus hemagglutinin. *Eur. J. Biochem., 205*(1), 147-153.

Kielian, M. (2006). Class II virus membrane fusion proteins. Virology, 344(1), 38-47.

Knipe, D.M., Howley, P.M. (Eds.). (2006). Fields Virology, Fifth Edition. New York: Lippincott Williams & Wilkins.

Krieger, F., Moglich, A., Kiefhaber ,T. (2005). Effect of proline and glycine residues on dynamics and barriers of loop formation in polypeptide chains. J. Am. Chem. Soc., 127(10), 3346-3352.

Kuhn, J. H., Becker, S., Ebihara, H., Geisbert, T. W., Johnson, K. M., Kawaoka, Y., Lipkin, W. I., Negredo, A. I. et al. (2010). Proposal for a revised taxonomy of the family Filoviridae: Classification, names of taxa and viruses, and virus abbreviations. *Archives of Virology 155*(12), 2083–2103.

Lakadamyali, M., Rust, M., Zhuang, X. (2004). Endocytosis of influenza viruses. Microbes Infect., 6(10), 929-936.

Lavillette, D., Ruggieri, A., Russell, S.J., Cosset, F.L. (2000). Activation of a cell entry pathway common to type C mammalian retroviruses by soluble envelope fragments. *J. Virol., 74*(1), 295-304.

Lazarowitz, S.G., Compans, R.W., Choppin, P.W. (1971). Influenza virus structural and nonstructural proteins in infected cells and their plasma membranes. *Virology, 46*(3), 830-843

Lee, J., Fusco, M., Hessell, A., Oswald, W., Burton, D., & Saphire, E. (2008). Structure of the Ebola virus glycoprotein bound to an antibody from a human survivor. *Nature, 454*, 177-182.

Lu, Z., Berson, J.F., Chen, Y., Turner, J.D., Zhang, T., Sharron, M., Jenks, M.H., Wang, Z., Kim, J., Rucker, J., Hoxie, J.A., Peiper, S.C., Doms, R.W. (1997). Evolution of HIV-1 coreceptor usage through interactions with distinct CCR5 and CXCR4 domains. *Proc. Natl. Acad. Sci. USA 94*, 6426-6431.

Maginnis, M.S., Forrest, J.C., Kopecky-Bromberg, S.A., Dickeson, S.K., Santoro, S.A., Zutter, M.M., Nemerow, G.R., Bergelson, J.M., Dermody, T.S. (2006). Beta1 integrin mediates internalization of mammalian reovirus. *J. Virol. 80*(6), 2760-2770.

Maginnis, M.S., Mainou, B.A., Derdowski, A., Johnson, E.M., Zent, R., Dermody, T.S. (2008). NPXY motifs in the beta1 integrin cytoplasmic tail are required for functional reovirus entry. *J. Virol. 82*(7), 3181-3191

Marsh, M., Helenius, A. (2006). Virus entry: Open sesame. *Cell 124*, 729-740.

Mercer, J., Helenius, A. (2009). Virus entry by macropinocytosis. *Nat. Cell Biol*. *11*, 510-520.

Mercer, J., Schelhass, M., Helenius, A. (2010). Virus entry by endocytosis. *Annu. Rev. Biochem. 79*, 803-833.

Mizra, A.M., Aguilar, H.C., Zhu, Q., Mahon, P.J., Rota, P.A., Lee, B., Iorio, R.M. (2011). Triggering of the newcastle disease virus fusion protein by a chimeric attachment protein that binds to Nipah virus receptors. *J. Biol. Chem., 286*(20), 17851-17860.

Moore, J.P., Kitchen, S.G., Pugach, P., Zack, J.A. (2004). The CCR5 and CXCR4 coreceptors-Central to understanding the transmission and pathogenesis of Human Immunodeficiency Virus Type 1 infection. *AIDS Research and Human Retroviruses, 20*(1), 111-126.

Murphy, F. (2010). Photograph. In M. Mitka, Experimental RNA therapy shows promise against Ebola virus. *JAMA, 304*(1), 868.

Nanbo, A., Masaki, Imai, M., Watanabe, S., Noda, T., Kei, T., Neumann, G., Halfmann, P., & Kawaoka, Y. (2010). Ebolavirus is internalized into host cells via macropinocytosis in a viral glycoprotein-dependent manner. *PLoS Pathogens, 6*(9), e1001121.

Nobusawa, E., Aoyama, T., Kato, H., Suzuki, Y., Tateno, Y., Nakajima, K. (1991). Comparison of complete amino acid sequences and receptor-binding properties among 13 serotypes of hemagglutinins of influenza A viruses. *Virology, 182*, 475–485.

Pe'ery, T., Mathews, M.B. (2006). Viral conquest of the host cell. In D.M. Knipe and P.M. Howley, (Eds.) Fields Virology Fourth Edition, Philadelphia: Lippincott Williams & Wilkins, pp. 169–200.

Pelkmans, L., Kartenbeck, J., Helenius, A. (2001). Caveolar endocytosis of simian virus 40 reveals a new two-step vesicular transport pathway to the ER. *Nat. Cell Biol., 3*(5)*,* 473-483.

Pelkmans, L., Helenius, A. (2002). Endocytosis via caveolae. *Traffic, 3*, 311-320.

Racaniello, V.R. (1996). Early events in poliovirus infection: Virus-receptor interactions. Proc. Natl. Acad. Sci., 93, 11378-11381.

Rafalski, M., Ortiz, A., Rockwell, A., van Ginkel, L.C., Lear, J.D., DeGrado, W.F., Wilschut, J. (1991). Membrane fusion activity of the influenza virus hemagglutinin: interaction of HA2 N-terminal peptides with phospholipid vesicles. *Biochemistry, 30*(42), 10211-10220.

Russell, P.J., Hertz, P.E., McMillan, B. (Eds.) (2011). Biology: The Dynamic Science, Second Edition. New York: Brooks Cole.

Saeed, M.F., Kolokoltsov, A.A., Albrecht, T., & Davey, R.A. (2010). Cellular entry of ebola virus involves uptake by a macropinocytosis-like mechanism and subsequent trafficking through early and late endosomes. PLoS Pathogens, 6(9), e1001110.

Sauter, N.K., Hanson, J.E., Glick, G.D., Brown, J.H., Crowther, R.L., Park, S.J., Skehel, J.J., Wiley, D.C. (1992). Binding of influenza virus hemagglutinin to analogs of its cell-surface receptor, sialic acid: analysis by proton nuclear magnetic resonance spectroscopy and X-ray crystallography. *Biochemistry, 31*, 9609-9621

Schmid, S. (1997). Clathrin-coated vesicle formation and protein sorting: An integrated process. *Annu. Rev. Biochem., 66*, 511-548.

Schornberg, K., Matsuyama, S., Kabsch, K., Delos, S., Bouton, A., White, J. (2006). Role of endosomal cathepsins in entry mediated by the Ebola virus glycoprotein. *J. Virol., 80*(8), 4174-4178.

Sebestyén, M.G., Budker, V.G., Budker, T., Subbotin, V.M., Zhang, G., Monahan, S.D., Lewis, D.L., Wong, S.C., Hagstrom, J.E., Wolff, J.A. (2006). Mechanism of plasmid delivery by hydrodynamic tail vein injection. I. Hepatocyte uptake of various molecules. *J. Gene. Med., 8*(7), 852-873.

Sieczkarski, S.B., Whittaker, G.R. (2005). Viral entry. In M. Marsh (Ed.) Membrane trafficking in viral replication. New York: Springer-Verlag.

Skehel, J. J., Waterfield, M.D. (1975). Studies on the primary structure of the influenza virus hemagglutinin. *Proc. Natl. Acad. Sci., USA 72*, 93-97.

Skehel, J.J., Bayley, P.M., Brown, E.B., Martin, S.R., Waterfield, M.D., White, J.M., Wilson, I.A., Wiley, D.C. (1982). Changes in the conformation of influenza virus hemagglutinin at the pH optimum of virus-mediated membrane fusion. Proc. Natl. Acad. Sci, 79, 968-972.

Smith, J.G., Cunningham, J.M. (2007). Receptor-Induced Thiolate Couples Env Activation to Retrovirus Fusion and Infection. *PLoS Pathogens, 3*, 1971-1981.

Spear, P.G., Longnecker, R. (2003). Herpesvirus entry: An update. *J. Virol., 77*(19), 10179-10185.

Sullivan, N., Sun, Y., Sattentau, Q., Thali, M., Wu, D., Denisova, G., Gershoni, J., Robinson, J. Moore, J., Sodroski, J. (1998). CD4-induced conformational changes in the Human Immunodeficiency Virus Type 1 gp120 glycoprotein: Consequences for virus entry and neutralization. *J. Virol., 72*(6), 4694-4703.

Takada, A., Robinson, C., Goto, H., Sanchez, A., Murti, K.G., Whitt, M.A., Kawaoka, Y. (1997). A system for functional analysis of Ebola virus glycoprotein. *PNAS, 94*(26), 14764-14769.

Tatulian, S.A., Hinterdorfer, P., Baber, G., Tamm, L.K. (1995). Influenza hemagglutinin assumes a tilted conformation during membrane fusion as determined by attenuated total reflection FTIR spectroscopy. *EMBO, 14*(22), 5514-5523.

Watowich, S., Skehel, J.J., Wiley, D.C. (1994). Crystal structures of influenza virus hemagglutinin in complex with high-affinity receptor analogs. *Structure, 2*, 719–731

White, J.M., Delos, S. E., Brecher, M.B., Schornberg, K. (2008). Structures and mechanisms of viral membrane fusion protein. *Crit. Rev. Biochem. Mol. Biol., 43*(3), 189-219.

Wiley, D.C., Skehel, J.J. (1987). The structure and function of the hemagglutinin membrane glycoprotein of influenza virus. *Annu. Rev. Biochem., 56*, 365-394.

Wilson, I.A., Skehel, J.J., Wiley, D.C. (1981). Structure of the haemagglutinin membrane glycoprotein of influenza virus at 3 A resolution. *Nature*, *289*, 366-73.

Wool-Lewis, R.J., Bates, P. (1998). Characterization of Ebola virus entry by using pseudotyped viruses: Identification of receptor-deficient cell lines. J.Virol, 72(4), 3155-3160.

Wool-Lewis, R.J., Bates, P. (1998). Characterization of Ebola virus entry by using pesudotyped viruses: Identification of receptor-deficient cell lines. *J. Virol., 72*(4), 3155-3160.

Young, J.T.Y. (2001). Virus entry and uncoating. In D.M. Knipe and P.M. Howley, (Eds.) Fields Virology Fourth Edition, Philadelphia: Lippincott Williams & Wilkins, pp. 87–103.